Marine and Petroleum Geology 163 (2024) 106771

Contents lists available at ScienceDirect

Marine and Petroleum Geology

journal homepage: www.elsevier.com/locate/marpetgeo

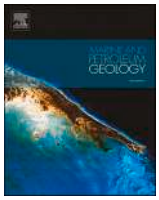

Structural control on carbon emissions at the Nirano mud volcanoes – Italy

B.M.S. Giambastiani [a], E. Chiapponi [a], F. Polo [a], M. Nespoli [b], A. Piombo [b], M. Antonellini [a,*]

[a] Department of Biological, Geological, and Environmental Sciences, Ravenna Campus, University of Bologna, Bologna, Italy
[b] Department of Physics and Astronomy "Augusto Righi", University of Bologna, Bologna, Italy

A B S T R A C T

The *Nirano Salse* in Italy is a well-studied site where natural gas seepage (NGS) and other hydrocarbon fluids and gases are emitted at the earth's surface. A novel integrated approach is applied to define a comprehensive structural interpretation of the gas seepage and flow dynamic in the mud volcano system of the *Nirano Salse* Regional Nature Reserve (Modena, Northern Apennines). The paper investigates the relationship between gas emissions and local structures, particularly faults and fractures, in the shallow subsurface (down to 500–600 m depth) to understand the control that structures have on fluid ascent from deep leaky hydrocarbon traps. We performed continuous monitoring of mud levels within vents; carried out geological surveys to characterize the main stratigraphic and structural discontinuities; measured the carbon emissions (CH_4 and CO_2) seepage both from volcanoes and the surrounding soil by a portable gas fluxmeter; and integrated the results with available geophysical surveys. The authors argue that the transgressive Pleistocene-Pliocene *Argille Azzurre* Formation hides the complex and highly structured pre-Pliocene geology of the area, in which faults and fractures act as pathways for deep fluid ascent. The emissions are aligned along a NE-SW trend at the intersection of a NE-SW fracture system and NW-SE-oriented normal faults, which are both associated to the local tensional stress field of a likely left-lateral strike-slip transfer structure or in the extrados of a fold. By examining both natural gas macroseepage and diffuse flux, it is shown that local structures control the fluid ascent and contribute to the emission of hydrocarbon gases and fluids at the Earth's surface. Understanding the structural control of carbon emissions at the *Nirano Salse* is also important for evaluating the carbon budget at the site, particularly in areas where there are detectable surface emissions. The study has implications for geologic, environmental, and economic issues, including hydrocarbon exploration, hazard assessment, and impact on the atmospheric carbon budget. Furthermore, the outcomes have an important implication to evaluate the potential for dangerous abrupt mud eruptions, and the site safety in proximity to the mud volcanoes.

1. Introduction

Natural gas seepage and venting at the Earth's surface associated with mud and other hydrocarbon gases and fluids are common phenomena in different kinds of geological environments such as thrust belts, geothermal areas, and high rate sedimentation and subsidence basins (Etiope, 2015; Etiope and Milkov, 2004; Kopf, 2002). With increasing awareness of the effects of greenhouse gases on the currently established climate warming trends (IPCC, 2022), it has become a pressing matter to characterize natural methane (CH_4) and associated gas and fluid emissions to establish their relevance in the carbon budget as well as to evaluate potential risks for the population living in areas where these phenomena are present. Furthermore, the connection between structural traps in the subsurface and hydrocarbon (gas/fluid) seepage at the Earth's surface is well established in the literature (Aminzadeh et al., 2013). Processes of mud diapirism and intrusion along faults, fold axes, and fracture zones, which are associated with gas and mud venting have been reported by MacDonald et al. (2000), Orange et al. (1999), Wang et al. (2022), and Zhong et al. (2021) in different parts of the world.

Gas seepage and emissions at the Earth's surface may be related to different phenomena and processes. In petroleum geology natural gas seepage is considered a hydrocarbon-rich gas mostly composed of methane deriving from the thermal maturation of organic source rock (Mazzini and Etiope, 2017). Natural gas, however, can also develop in abiotic conditions during igneous rock emplacement, metamorphism, and geothermal conditions (Etiope and Sherwood Lollar, 2013). Biogenic methane development is also another important process at the Earth's surface during sediment diagenesis and is the physiologic product of microbial communities active at low environmental temperatures (60–80 °C) (Formolo, 2010; Hunt, 1996).

According to Etiope et al. (2011) and Etiope (2005) localized and channelled venting of natural gas from mud volcanoes, bubbling mud pools, and gryphons is named "macro-seep", whereas pervasive widespread dispersed exhalation through pores and microfractures of sediments and rocks throughout relatively large areas, conceptually independent from macro-seep, is referred to as "microseepage". Another seepage, named 'miniseepage', occurs that defines the invisible, diffuse exhalation of gas from the muddy ground surrounding pools and gryphons, by identifying a transition area of tens or hundreds of meters

* Corresponding author.
E-mail address: m.antonellini@unibo.it (M. Antonellini).

https://doi.org/10.1016/j.marpetgeo.2024.106771
Received 24 October 2023; Received in revised form 22 February 2024; Accepted 23 February 2024
Available online 24 February 2024

surrounding the macro-seepage zone, where gas gradually decreases. Micro and miniseepage are both governed by gas diffusion. Natural gas and fluids macro-seepage, on the other hand, is governed by advective and density difference transport along pipes and open fracture zones (Wan et al., 2021).

Natural gas seepage (NGS from now onward) has implications for several geologic, environmental, and economic issues. In geology, NGS indicates tectonic discontinuities and fracture permeability whereas in hydrocarbon exploration it has always been considered a convenient means to sample and geochemically assess the fluids of the petroleum system before exploitation or to individuate leaky seals (both for hydrocarbons and CO_2 storage) in the subsurface. NGS is a hazard to humans and constructions especially during explosive surface venting or for the degradation of soil characteristics next to focused emission points or for the pollution of aquifers and rivers (Mazzini and Etiope, 2017). NGS may have a significant impact on the atmospheric carbon budget and its contribution needs to be assessed at the local and global scale for completion of required inventory sources of carbon. There are large discrepancies between the estimates of natural methane sources by Hmiel et al. (2020) and other studies (Mazzini et al., 2021b) also conducted on specific geological sources such as mud volcanoes macro-seeps in the same geographical area and at global level. Methane gas may have contributed to past climate change events by changing the concentrations of greenhouse gases in the atmosphere. Methane, in fact, is a much more powerful greenhouse gas than CO_2 (Howarth, 2014). Furthermore, NGS, where associated with fire at the surface, is important to many cultures that revere these phenomena in the context of the Zoroasther cult (Amrikazemi and Mehrpooya, 2005; Kuhn, 2000; Leroy et al., 2022). Finally, but not least, the economic exploitation of mud seeps for geotourism has become an important business for the recreational and medical properties of mud baths (Herrera-Franco et al., 2020; Madeja and Mrowczyk, 2010).

In this paper, we investigate the relationships between gas emissions and local structures in the *Nirano Salse* (Italy), which is a well-studied site where geochemical, geophysical, and structural data are available (Bonini, 2007, 2008, 2009; Giambastiani et al., 2022; Heller et al., 2011, 2012; Lupi et al., 2016; Martinelli and Rabbi, 1998; Nespoli et al., 2023; Romano et al., 2023; Sciarra et al., 2019). We examine both natural gas macro-, mini- and micro-seepages for relating their venue to structural elements such as faults and fractures. The objective of our work is to show that local structures control fluid ascent in the shallow subsurface (depth down to 500–600 m) from deep leaky hydrocarbon traps developed in a thrust fold tectonic setting. The reason to study the relationships between gas emissions and structures has multiple purposes. The

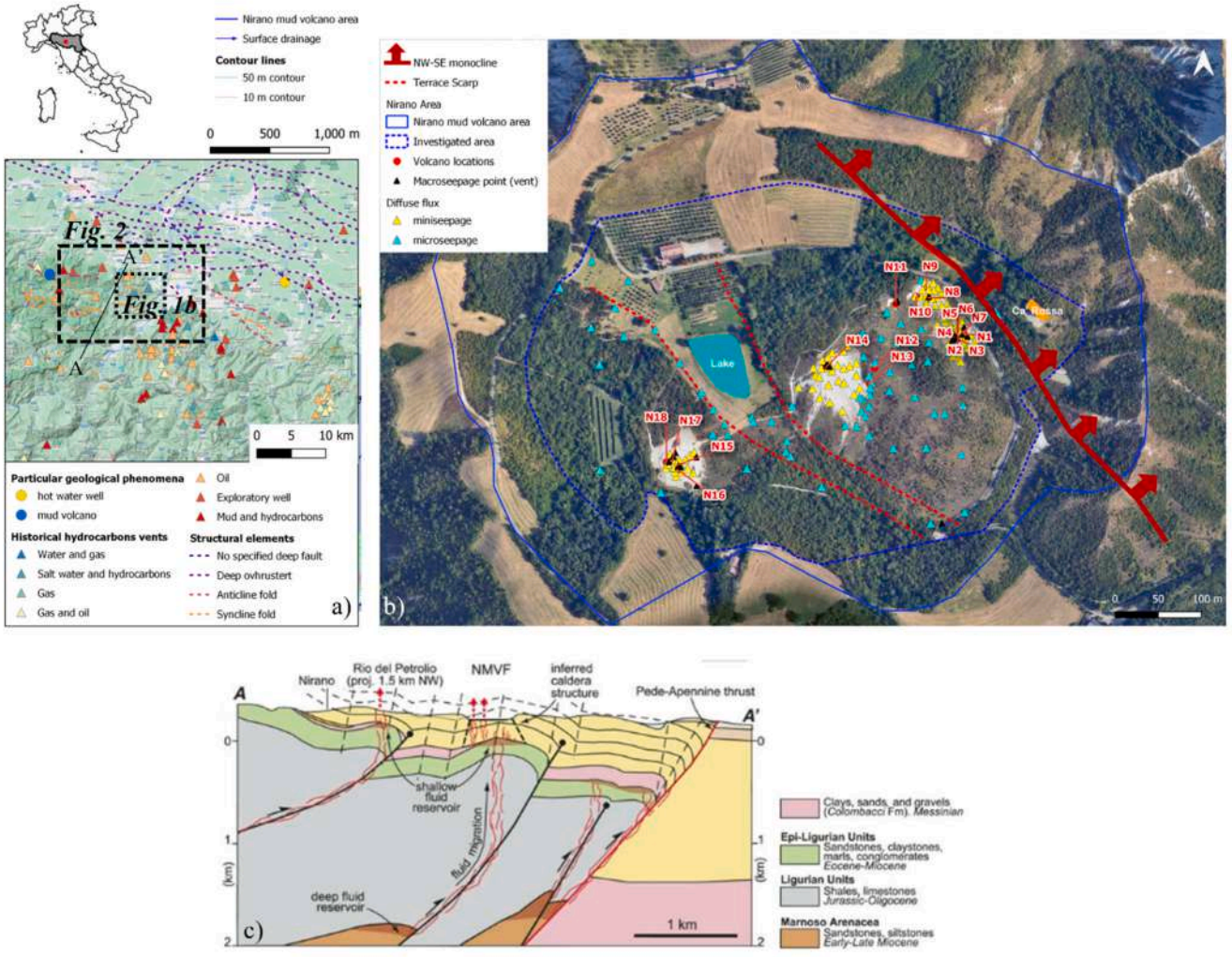

Fig. 1. Location of the *Nirano Salse* study area. a) The geological phenomena and historical hydrocarbons vents that occurred in the surrounding area (modified from Giambastiani et al., 2022); b) location of gryphons and mud pools (red dots), gas measurement points (black triangles for macroseepage; yellow ad cyan triangles for mini- and micro-seepage, respectively). Coordinate reference system: WGS 1984 UTM Zone 32N). c) Schematic cross section (trace in Fig. 1a) at regional level showing the deep sources and potential migration pathways as proposed by Bonini (2007) and modified from Sciarra et al. (2015).

first is to accurately evaluate the carbon budget at the site focusing on areas where detectable surface emissions are; in the second instance, to evaluate the hazards at specific positions in the site, so that better and safer routes can be devised for the tourists visiting the area in a way to avoid sudden mud explosions, dangerous gas concentrations, and soil sinking; finally, to highlight how the integration of geophysical and structural geology techniques can aid in pinpointing the processes controlling gas and mud venting at the earth surface.

1.1. Structural setting

The study area (Fig. 1a) is located within the outcropping surface front of the Northern Apennines (Italy), specifically in the Regional Nature Reserve of the *Nirano Salse* (hereafter referred to as *Nirano Salse*). This area has been known since historical times (Bonini, 2020; Manga and Bonini, 2012) for its cold seeps of salty connate water mixed with clay, liquid hydrocarbons, and gas emissions. Gryphons, mud pools, and dry seeps are spread over an area of about 40 ha within a hilly Badlands landscape (Figs. 1 and 2).

Morphologically, the area is shaped like an oval depression with a diameter of 800 m, which has led some authors to propose the existence of a mud caldera and a collapsed structure or of a gravitational collapse above a mud diapir in the Plio-Pleistocene (Bonini, 2008, 2009; Oppo et al., 2013; Sciarra et al., 2019). However, the bottom of the depression is also divided into three benches trending E-W to NW-SE, down-stepping to the north where the three major mud volcano groups are located (Fig. 1b). The shape of the mud and gas vents depends on the type of emissions: irregular, discontinuous, and explosive gas-mud emissions tend to form gryphons, whereas quiet, continuous emissions form mud pools (Mazzini et al., 2021a,b). The largest gryphons have basal diameters of 4–5 m, rims with diameters of 0.2–2 m, and heights of 2–3 m above ground (Fig. 2). The emissions consist of intermittent gas bubbles and muddy water with variable flow rates. Generally, there is a continuous supply of small bubbles (about a few cm in diameter), but their frequency may vary, and every few minutes larger bubbles break the surface, especially in the most active gryphons of the central area. The wireline sounding depth of the conduits down to the shallow buffer reservoirs within the *Argille Azzurre* Fm ranges from 0.6 to 5 m for the gryphons, whereas the depth of mud pool conduits ranges from 8 to 15 m, suggesting a straighter, more vertical, pipe-like structure in the latter (Giambastiani et al., 2022 and Fig. 11c therein). The shallow reservoirs in the *Argille Azzurre* Fm and/or just below its base are shallow buffer reservoirs that accumulate gas coming from a much deeper source (Fig. 1c) within a thrust-controlled anticlinal trap in the Tortonian *Marnoso Arenacea* Fm at a depth of about 2500 m (Bonini, 2007).

Fig. 2. The hilly landscape and the typical morphology of the mud vents in the *Nirano Salse* study area. At the forefront a mud pool with a 9 m deep conduit and at the back a few gryphons.

1.2. Geologic and stratigraphic setting

The Plio-Pleistocene *Argille Azzurre* Formation (Fm) is outcropping in the whole area of the *Nirano Salse* (Fig. 1S in Suppl. Mat. and stratigraphic sequence in Fig. 4). The *Argille Azzurre* Fm primarily consists of marine clays, with sandy and conglomerate layers occurring only at their base near the transgression over the Messinian *Colombacci* Fm and the Epiligurian sequence (Amorosi et al., 1998).

The Epiligurian Sequence can be divided into several main units, which from top to bottom include the Tortonian-Messinian *Termina* Fm composed of sandy marly sediments with a thickness exceeding 500 m. The Burdigalian-Serravallian marls and marly turbidites of the *Bismantova* group (*Cigarello* and *Pantano* Fms) occur below the *Termina* Fm and have a thickness of about 400 m. The Rupelian-Burdigalian marls of the *Contignaco* and *Antognola* Fm have a variable thickness (50–500 m) just below the *Bismantova* Group. The Lutezian-Rupelian *Montepiano-Loiano-Ranzano* Fm with mostly high porosity sandy conglomeratic sediments intercalated with clays have a thickness of about 500 m and form the base of the Epiligurian sequence. Below the Epiligurian, the Cretaceous to Eocene chaotic Ligurian mélange complex and the associated *Baiso* breccias form the base of the Tertiary sequence (Gasperi et al., 2005).

1.3. Tectonics

There are no clearly mapped faults in the *Argille Azzurre* Fm (FAA), as evidenced by Gasperi et al. (2005) and Fig. 1a. As folding is present in some areas, brittle structures are relatively few in the clays. In contrast, the Miocene-Eocene sequence below the transgression is intensely faulted and fractured, with prevalent NW-SE and NE-SW structural trends. These trends are common in the Northern Apennines, as noted by Gasperi et al. (2005), Carlini et al. (2016), and Mariucci et al. (1999).

The published geological map (Gasperi et al., 2005) and some authors (Bonini, 2008, 2009, 2020; Maestrelli et al., 2019) describe a NW-SE anticline axis crossing the *Nirano Salse* area. Our field observations, however, do not recognize this feature but the axis of a NW-SE monocline (strata dipping NE north of the monocline), which marks the area of steepening of the FAA strata to the NE (Fig. 1b). Mud volcanoes are aligned along a NE-SW line, which is close to the contractional direction in the tectonic context of the Northern Apennines, and thus to the maximum current in-situ stress orientation (S_H) (ENE-SSW according to Serpelloni et al., 2015). Gas emissions are interpreted as surface expressions of fluids escaping from a deep leaky reservoir located below the Ligurian complex (at a depth of around 2.5 km). Leakage from a top membrane or fault seal in the deep reservoir could facilitate the rise of gas along faults and fractures into the fractured Epiligurian units (800–1200 m deep) of Eocene-Miocene age, and via fingering in the upper Plio-Pleistocene ductile clays.

Seismic events in this section of the Northern Apennines are primarily due to thrusting (with magnitudes ranging from 3.0 to 4.0) and in the Ped Apennines and the Po Plain also by strike-slip faulting (with magnitudes ranging from 3.5 to 5) (Bonini, 2009, 2008; Bennett et al., 2012; INGV website: https://terremoti.ingv.it/).

1.4. Mud and fluids origin and characterization

The emissions at the vents of the *Nirano Salse* consist of a mix of cold brackish water, clay, gases (CH_4 and CO_2), peat fragments, and traces of liquid hydrocarbons. Mud is formed in the conduits by the continuous gas bubbling which mixes the liquid phase (brackish water) with the clay of the conduit walls. Mud expulsion at the surface, therefore, is driven by the adiabatic expansion of the gas bubbles during their ascent in the conduits. A different gas/liquid ratio is present in each conduit, so the mud level is different in each vent; higher levels correspond to

gryphons where the volcanism is more explosive, and the gas/liquid ratios are large (Giambastiani et al., 2022). Accumulation of gas in shallow aquifers within permeable layers of the *Argille Azzurre* Fm or at contact with the Miocene rocks decreases fluid density and increases the overpressure, which allows the fluids to rise at the surface (Martinelli et al., 2012; Mattavelli et al., 1983; Mattavelli and Novelli, 1988).

Several authors (Martinelli et al., 2012; Mattavelli et al., 1983, 1993; Riva et al., 1986) affirm that the hydrocarbons in this region of the Northern Apennines formed in the turbiditic Miocene *Marnoso Arenacea* Fm, which, in this area, lays below the chaotic Ligurian Complex. Some more recent studies (Bonini, 2009; Capozzi and Picotti, 2002, 2010; Oppo et al., 2013; Picotti et al., 2007), however, suggest that the source rock for these hydrocarbons could be located even deeper, possibly in Triassic source rocks (Sciarra et al., 2019). Despite this, micropaleontological analysis of mud samples collected from the *Nirano Salse* vents indicates that the phoraminiphera and benthic fossils in the mud all belong to the Plio-Pleistocene *Argille Azzurre* Fm (Papazzoni, 2017).

The brackish waters making up the mud are likely to be connate pore marine entrapped in the Plio-Pleistocene sediments as supported by the isotopic signatures of δD and $\delta^{18}O$ (Conti et al., 2000; Heller et al., 2011; Martinelli and Judd, 2004; Minissale et al., 2000; Oppo et al., 2013; Sciarra et al., 2019). Geochemical studies on gas and water samples have also revealed that the gas consists of a mixture of primary and secondary thermogenic gases due to thermal cracking of oil, biogenic CH_4 due to biodegradation of oils, with minor condensates and oil (Oppo et al., 2017; Tassi et al., 2012).

Geochemical and isotopic investigations by Sciarra et al. (2019) on the gases exiting the vents confirm a thermogenic origin for the methane originating from organic material at temperatures higher than 100 °C (Whiticar and Suess, 1990). Sciarra et al. (2019) also analyze the CO_2 isotopes and suggest that the strongly positive $\delta^{13}C$–CO_2 indicates that the CO_2 is caused by anaerobic oxidation of heavy hydrocarbons (Pallasser, 2000), followed by secondary methanogenesis (Tassi et al., 2012). This process depends on the reservoir microbial communities, as well as its pressure-temperature conditions, and can strongly enrich the residual CO_2 in ^{13}C (Etiope et al., 2009; Wang et al., 2005).

2. Methodology

Different geological, hydrogeological, and geochemical techniques were integrated and used to characterize the relationships between gas emissions and structures at the *Nirano Salse*.

2.1. Field geology

Field mapping allowed to check the existing geological maps (Bonini, 2012; Gasperi, 1989; Gasperi et al., 2005) and integrate them with new structural observations (attitude of strata and fault traces) and interpretations derived by geophysical data. Rose diagrams with the trends of the principal faults reported in the geologic map and observed in the field were constructed with the Stereonet 11 software (Allmendinger, 2019). The rose diagrams report major fractures and fault traces identified only in the Ligurian and Epi-Ligurian units, because the *Argille Azzurre* Fm are ductile clay units and do not show a brittle behaviour resulting in observable lineaments. Geological cross-sections were also drafted using the updated geological maps and the geophysical data.

All data were interpreted with regard to the geological information available for the area, such as penetrometer, cores, and well logs data from the archive of the ViDEPI project database (https://www.videpi.com/videpi) concerning Italian oil exploration within the National Mining Service for Hydrocarbons and geothermal energy of the Italian Ministry for Economic Development available for the area and recent studies (Giambastiani et al., 2022).

2.2. Hydrogeological methods

Three gryphons (N14, N3, and N1, refer to Fig. 1b for the location) were equipped with level-loggers LTC Solinst to monitor mud hydrostatic pressure, temperature (T), and electrical conductivity (EC). The probes were installed at a depth of 3.0 m from the surface, and parameters were recorded at 1-sec intervals for a total of 1 h.

The pressure variations recorded by the probe correspond to the transit of a gas bubble in the mud column. The bubble frequency was based on the count of all positive oscillations of hydrostatic pressure over the monitored time, while the total volume of emissions was calculated assuming an average diameter of 5 cm for the bubbles (based on field observations and the inner diameter of the three conduits) and a variable height equivalent to the pressure variation measured in the conduit. Using the ideal gas equation, the volume was converted into molar volume at conditions of 15 °C and 1 atm. Emissions and bubble frequency were considered an indicator of the vent activity and were compared and discussed about the measured gas fluxes.

2.3. Gas geochemistry

Gas diffusion (micro- and mini-seepages) from soil and direct gas emissions from the volcano vents (macroseepage) were measured during 3 campaigns from June to December 2022 for a total of 190-point fluxes observations. Gas measurements from soil (94 and 69 points for miniseepage and microseepage, respectively, for a total of 163 points, 86% of dataset) and direct gas from mud pools and gryphons (27 points, 14% of dataset) were performed by a portable CH_4–CO_2 flux-meter (West Systems srl, Pontedera, Italy) equipped with two infrared spectrophotometer detectors (Licor 8002 for CO_2, and tunable laser diode with multipass cell for CH_4) and wireless data communication to a palm-top computer; the gas fluxes were automatically calculated through linear regression of the gas concentration build-up on the chamber. Within the three major mud volcano groups in Fig. 1b, as miniseepage, we considered the gas exhalation within 50 m from each volcanic vent and pool, while microseepage is considered only as gas exhalation from the soil in the vegetated areas away from volcanic vents and, thus, independent from macroseepage. The accumulation chamber is of type A with a net volume of 0.003 m^3, base area of 0.03 m^2, and internal height of 98 mm, providing a rotating vent to avoid stratification inside the chamber. All measurements were retrieved using the closed-chamber system and recording measurements across the whole volcano field and surroundings (Fig. 1c), depending on the environmental conditions and field accessibility, covering a total area of 40.3 ha. Points were 10 m spaced on average and were georeferenced by a real-time kinematic differential global positioning system (RTK-DGPS).

Gas flux measurements were based on the accumulation chamber "time 0" method (Capaccioni et al., 2010, 2015; Cardellini et al., 2003). Based on the linear regression of increased CH_4 and CO_2 concentration values over time inside the dark chamber, fluxes from a single point source were estimated, using the Flux Revision Software produced by West System s.r.l. (Giovenali et al., 2013). All measurements have been recorded after a minimum of 90 s of analysis. Based on the CH_4 detector specifications, the precision depends on the measurement flux (±25% for a flux range of 0.2–10 mol/m^2/d; ±10% for a flux range of 10–600 mol/m^2/d). Measurement of very low CH_4 fluxes (<0.2 mol/m^2/d) is still possible but the error increases due to the low detector sensitivity (West Systems, 2012); thus, a value of 0.10 mol/m^2/d was assigned to all positive CH_4 fluxes ≤0.2 mol/m^2/d. Gas fluxes were corrected by using atmospheric pressure and air temperature data recorded by the weather station of Vignola (Modena) and available from the Regional Agency for Prevention, Environment, and Energy of Emilia-Romagna (ARPAE website: https://simc.arpae.it/dext3r/).

The annual flux budget from an individual vent (g/m^2/d) was calculated from the flux measured by the closed-chamber (g/m^2/d) multiplied by the chamber area (0.03 m^2), which corresponds to or is

slightly smaller than the actual gas vent. The partial emissions budget for the muddy area surrounding the mud volcano vents (miniseepage) is obtained by multiplying the average flux (g/m^2/d) by the area of the three volcano group of about 1.1 ha (where yellow points in Fig. 1b are located). The exhalation that is far or independent from vents (microseepage) is obtained by multiplying the average flux (g/m^2/d) by the entire investigated area, excluding miniseepage area, for a total of about 20 ha (delimited by blue dashed line in Fig. 1b). The total annual gas emissions from the field (t/yr) were then obtained by the sum of all point sources (vents) plus the total output from diffuse seepage (Etiope et al., 2011). Total CO_2 equivalent (t/year) was estimated using the GWP (Global Warming Potentials) factor of 27.9 (IPCC, 2022). The volumetric ratio between CH_4 and CO_2 fluxes and the 'emission factor', expressed as the total measured output divided by the investigated seepage area (Etiope et al., 2007, 2011; Etiope et al., 2007a,b), were calculated.

The measured Greenhouse Gas Emissions (GHG from now on) emissions in Nirano were also evaluated in relation to regional and municipal (Modena, IT) emissions. The year 2020 GHG emissions were made available through the emissions inventory archive of ARPAE (https://www.arpae.it/it/temi-ambientali/aria/inventari-emissioni/inventario-emissioni-gas-serra/archivio-inventari-emissioni-ghg). This inventory follows the methodology of the IPCC, which divides the main emission sources and carbon storage into four main sectors: energy; industrial processes and product use (IPPU); agriculture, forestry, and other land uses (AFOLU), and waste.

To show the spatial variability, it was decided to consider diffuse flux and macroseepage separately due to their different variability, distributions, and orders of magnitude. The spatial analysis of CH_4 and CO_2 diffuse flux was performed using the point Kriging interpolation into the Surfer ® 15.6.3. software with a linear semi-variogram model with no drift, no nugget effect, and no circular search ellipse. Maps with contour lines of equal emissions were generated based on diffuse flux data expressed in g/m^2/d, using raw data instead of substituted data by the limit of detection. To assess the quality of the interpolation (goodness of fit), we calculated residual and R^2 values between estimated and measured values. The macroseepage flow was displayed on maps using symbols proportional to the flow rate of individual vents.

3. Results

3.1. Structural data

Fig. 3 reports the three geologic domains and fault trace directions in the segment of the Northern Apennines extending from the valley of the Secchia River in the west to the valley of the Panaro River in the east. The area is divided into three main domains: i) the oldest Ligurian domain in the south-west; ii) the Epiligurian domain in the central part; iii) and the youngest *Argille Azzurre* domain in the NE. The contact between the FAA and the Epiligurian domain is by transgression (base of the *Argille Azzurre* Fm or the Colombacci Fm), whereas the contact between the Epiligurian and Ligurian domains is tectonic or depositional. Bedding is mostly striking NW-SE in the *Argille Azzurre* domain with dips

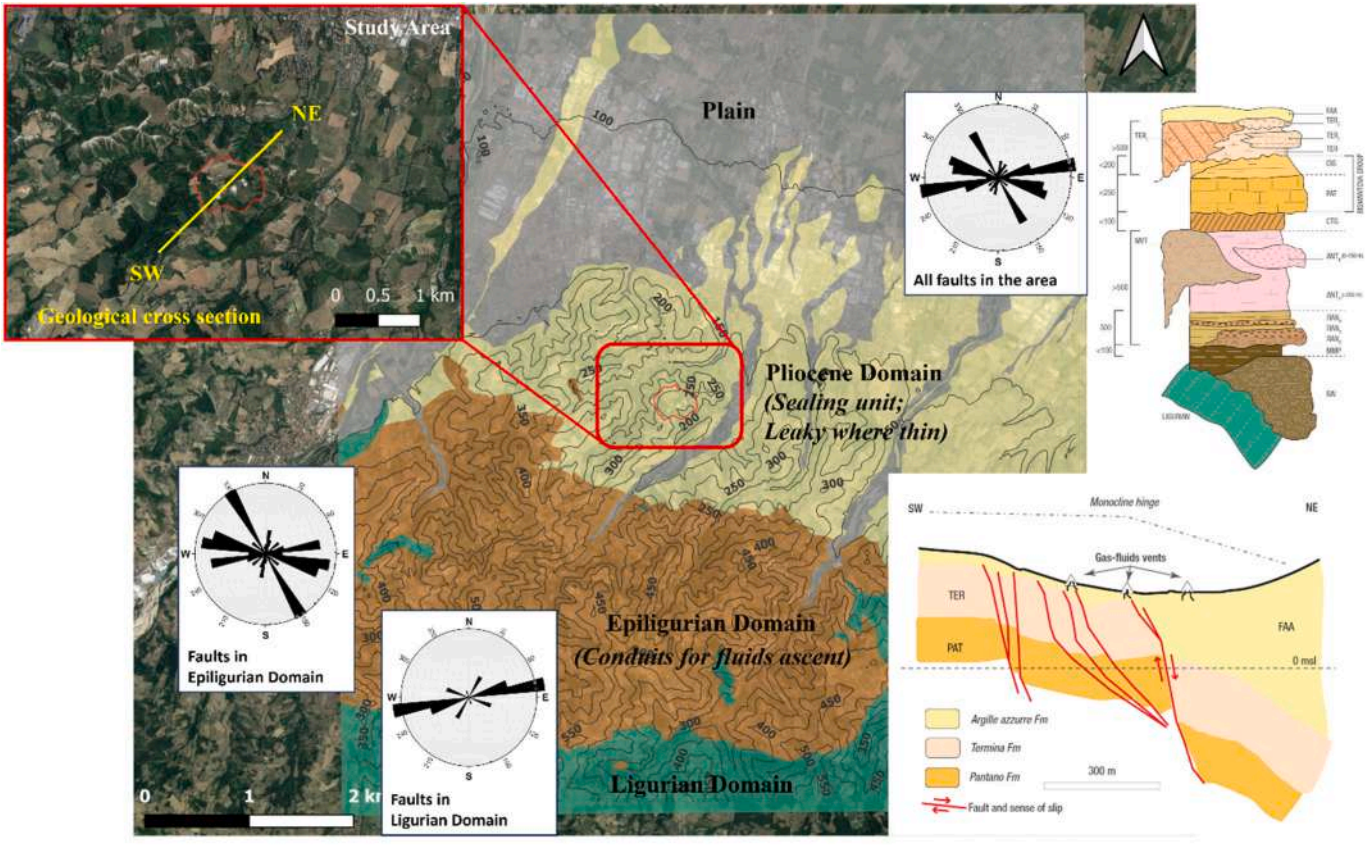

Fig. 3. –Geological domains (modified from the geological map of the Emilia-Romagna Region, scale 1:50000), along with the stratigraphic profile (details and legend in Fig. 1S in Suppl. Mat.) and reconstruction of a geological cross-section of the *Nirano Salse* area. The rose diagrams indicate the directions of faults and major fracture lineaments mapped in the area. The Epiligurian domain includes brittle units that are faulted and fractured and are the likely candidates for the presence of localized avenues of ascent for the deep fluids containing hydrocarbons. The Pliocene domain (*Argille Azzurre* Fm) includes only ductile units mostly made up of clay and some sandy levels more frequent at the base of the sequence. No faults and fractures are apparent within this domain that most likely act as a seal for gas and fluids ascending from depth. Where the Pliocene is thinner (southern part of the domain), the seal could be leaky, and the fluids reach the surface forming the mud volcanoes vents.

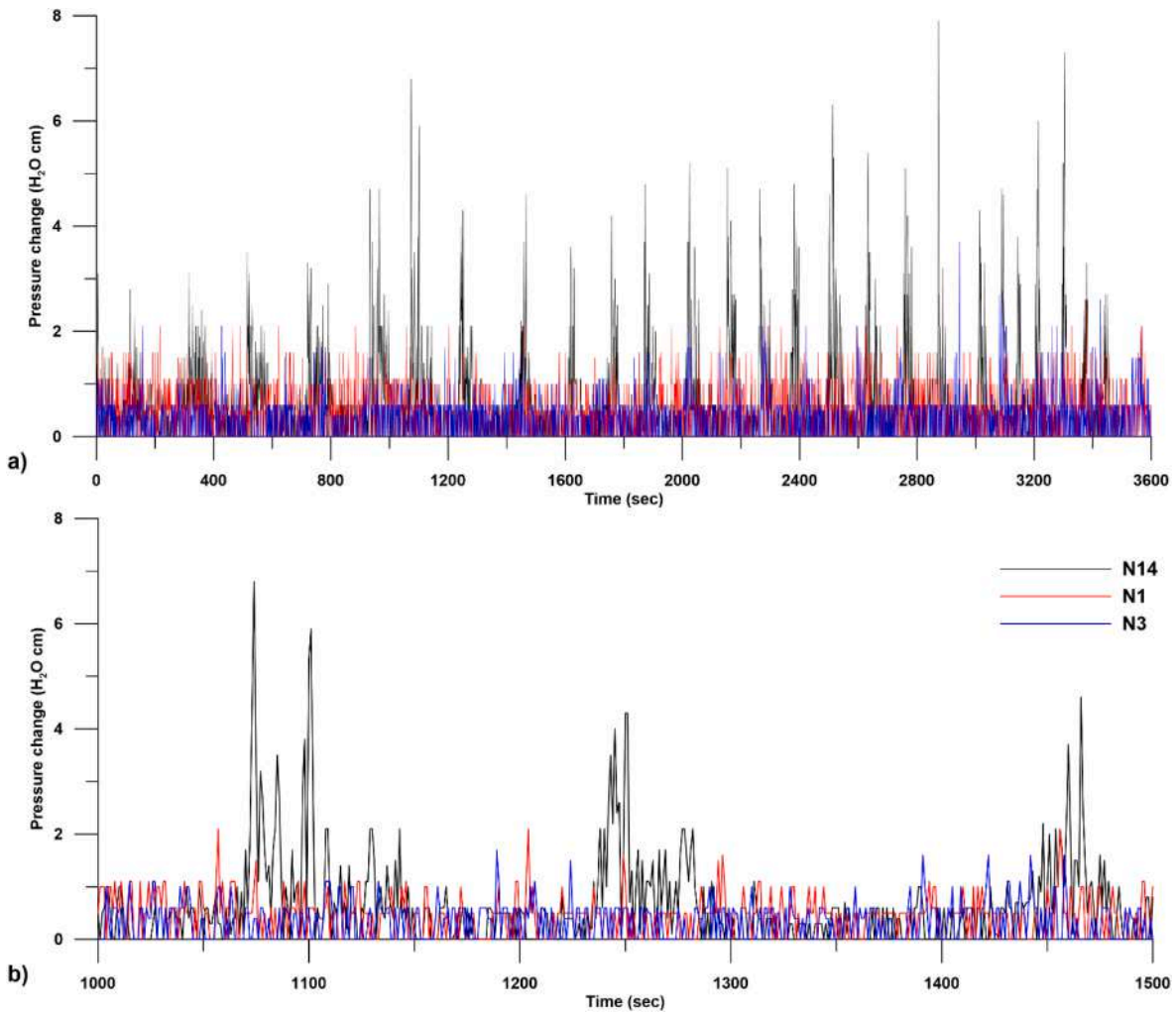

Fig. 4. (a) Pressure fluctuations due to gas bubble ascent in vents N14, N1, and N3 (1-h monitoring at 1 s time interval); (b) zoom of the figure (a) for an interval of 500 s.

from gentle (5–15°) next to the basal transgression to steep (35–50°) in the NE towards the Po plain. Strike and dip of the strata in the Epiligurian domain is generally NW-SE to the NE but there is a large variability due to the presence of many faulted blocks and the transgression at the base of the Messinian Termina Fm. Bedding in the Ligurian domain is chaotic and often overturned. Faults are rare in the *Argille Azzurre* domain and present only in the southwestern part, where the clays are thin (about 30–50 m). Faults in the Epiligurian domain have two distinctive trends (see inset in Fig. 3): the most conspicuous are the NW-SE one and the ENE-WSW one. There is some dispersion in the fault trends due to the block faulting typical of the Epiligurian domains as also remarked by Stendardi et al. (2023). Faults major trend in the Ligurian domain is E-W to ENE-WSW (see inset in Fig. 3) with little dispersion.

3.2. Hydrogeological data

Considering the pressure variations data in gryphons, we can distinguish two kinds of behaviour that are represented in Fig. 4: high frequency (0.7 Hz) pressure variations with small amplitudes (less than 1 mbar) form a background in most active vents (N3 and N1) with a short period of 1.5 s between gas bubbles and no pressure variation greater than 3 mbar; a periodic (80 s) high amplitude (>4 mbar, up to 7 mbar) signal which was observed only at vent N14. Visual inspection of the vents shows that the high frequency small amplitude signal is due to almost continuous ascent of small diameter (2–5 cm) gas bubbles whereas the long periodicity high amplitude signal is due to the ascent of large bubbles (40–50 cm in diameter) displacing several litres of mud from the conduit that then expands as a mud flow at the base of the gryphon.

Bubble frequency plots at 1 s sampling allow also to make carbon emissions estimates. For example, at the central mud vent N14 (with high amplitude low periodicity signal) and based on bubble frequency and size, the estimated CH_4 flux is 0.22 t/yr, which is equivalent to a flux of 6.3 CO_2-eq t/yr. At the mud pools N1 and N3 (with only high frequency small amplitude signal), we estimated a CH_4 flux of 0.18 and 0.12 t/yr, respectively, which is equivalent to about a flux of 5.1 and 3.5 CO_2-eq t/yr.

3.3. Gas emissions data

Table 2 shows the main statistical parameters of the measured gas emissions in the Nirano field, both direct emission from the mud volcano vents and the surrounding area in terms of diffusion (mini- and micro seepage).

Due to a wide range of values, high coefficients of variation, and skewness values, data are associated with an asymmetric distribution caused by the presence of various outliers, attributable to emissions from the sampled vents. The data of CH_4 diffuse flux shows an average of 2.27 g/m^2/d, with maximum value of 6.75 g/m^2/d, which is attributed to the presence of a dry seep emission in a fissure in the ground that is

Table 1
Frequency analysis of the gas bubbles ascent in vents N14, N1, and N3 (time series in Fig. 4).

ΔP (H_2O cm)	N14		N1		N3	
	N. events	Period (sec)	N. events	Period (sec)	N. events	Period (sec)
<1	2857	1	2331	2	2439	1
<2	377	9	1133	3	1107	3
<3	167	21	136	26	55	65
<4	59	59	#		#	
>4	40	88	#		#	
TOTAL	3500		3600		3600	

close to gryphon N9 (Fig. 1).

The collected data confirms that the macroseepage by the mud volcanoes is primarily composed of CH_4, with lesser amounts of CO_2 and an average CH_4/CO_2 ratio of 189. The total CH_4 flux emitted by the sampled mud volcano vents is approximately 5.71 t/yr whereas the flux of CO_2 is considerably smaller, with values of 0.13 t/yr. The muddy area surrounding the sampled vents emits approximately 42.30 t/yr of CO_2, and 9.04 t/yr of CH_4 with an average CH_4/CO_2 ratio of 2.90. CH_4 and CO_2 microseepage is about 164.49 t/yr and 1698.92 t/yr, respectively, with an average CH_4/CO_2 ratio of 1.01. In the Nirano area, the estimated GHG emissions are approximately 0.01 $MtCO_2$-eq/yr (Table 2).

Maps of CH_4 and CO_2 fluxes obtained by kriging interpolation with grid size 5 × 5m are shown in Fig. 5. R^2 values are 0.7 and 0.6 for CH_4 and CO_2 interpolation, respectively.

From the CH_4 maps (Fig. 5a), high emission macroseepage (circles >2 10^5 g/m^2/d) can be observed in the southwestern parts, corresponding to one of the three major mud volcano systems in the area. There are also clusters with anomalous values (~4 10^3 g/m^2/d) that appear to align NE-SW across the volcano field. The CH_4 diffuse flux map highlights the presence of two anomalous alignments. The first one is in the eastern sector with a NE-SW direction, which passes west of Ca' Rossa and extends south of N12 where high values are measured (6 g/m^2/d). The other alignment almost longitudinally crosses the entire central area affected by mud volcanoes, starting from vent N9 throughout N12 and extending west of the field, always following the same direction (NE-SW). The highest values of CH_4 diffuse flux are located on the eastern part, associated with an area with dry soil and evident cracks, whereas the emissions measured outside the surface venting range between 0 and 1.2 g/m^2/d.

In the CO_2 emission rate maps (Fig. 5b), a sector with high macroseepage values (>2.2 10^3 g/m^2/d) compared to the surrounding area can be observed; it is located in the southern part near the N15 volcano. Additionally, there is a positive anomaly in the NE part of the reserve, near Cà Rossa where the mud volcano activity is more recent, with CO_2 emission of 1.6 10^3 g/m^2/d. Maximum CO_2 microseepage is measured outside the surface venting, in the vegetated area around the field, with an average value of about 30 g/m^2/d; an area characterized by high values (average of about 46 g/m^2/d and maximum of 90 g/m^2/d) is found in the NW part, corresponding to the small lake and a morphological slope.

4. Discussion

4.1. Gas emissions

Total CH_4 emission from Nirano is estimated to be about 179 t/yr of which more than 90% is from invisible seepage surrounding the mud volcano vents. The order of magnitude of emissions recorded in the *Nirano Salse* is generally consistent with other research conducted in the area. Etiope et al. (2007a,b) and Sciarra et al. (2019) have also estimated the CH_4 production from macroseeps (vents, pools, and dry emissions) and microseeps (diffusion from the soil) in Nirano. According to Etiope et al. (2007a,b), individual mud volcano vents in Nirano contribute approximately 0.3 t/yr, with a total macroseepage of 6 t/yr, while Sciarra et al. (2019) estimated a total of 4.72 t/yr. The CH_4 macroseep estimates obtained in this study (0.2 t/yr for the individual vent and 6 t/yr for the total seepage) align with these estimates. However, regarding average CH_4 microseep output, the total output recorded in the present study (164.5 t/yr) is higher than the one obtained by Etiope et al. (2007a,b) equal to 26.4 t/yr, and one order of magnitude higher than the one by Sciarra et al. (2019) (2.13 t/yr).

The observed differences may be attributed to (Oertel et al., 2016). 2) Different sampling densities (Ciotoli et al., 2007): 210 measurements in 8 ha in Sciarra et al. (2019) and 6 measurements in 1 ha in Etiope et al. (2007a,b) vs 69 measurements in 20 ha for our study). The monitored area is a multiplicative factor in calculating diffuse flux, thereby influencing the final budget. The selected area was chosen by encompassing all microseepage points and following the 240 m a.s.l. contour line, including the vegetated areas around the field and considering the geomorphology. Moreover, as evident in Table 2, the dataset shows high coefficients of variation (typical for gas flux measurements), indicating high data dispersion relative to the mean value and making large scale estimates more challenging. 3) The use of various techniques for determining the gas output (e.g. inverted bottles; calibrated plot of bubble flux vs. bubble size vs. bubble frequency, wet test gas flow meter, and closed method) may lead to different discrepancies in the results due to differences in measurement principles, sensitivities, and potential sources of error associated with each method (Etiope et al., 2011). 4) As mentioned above and in Giambastiani et al. (2022), the gas alimentation from the depth is not constant over time and the mud emissions are continuously evolving along with the specific number and location of

Table 2
Statistics of direct gas emission from the vents (a) and gas seepage from the soil (b). Reported is also the partial and total annual gas budget for the Nirano field. (Note: CV is for coefficient of variation; SD is for standard deviation; * surveyed area = 1.1 ha; § surveyed area = 20 ha).

	Vents (g/m^2/d)			Miniseepage (g/m^2/d)			Microseepage (g/m^2/d)		
	CH_4 (g/m^2/d)	**CO_2** (g/m^2/d)	**CH_4/CO_2** (vol.)	**CH_4** (g/m^2/d)	**CO_2** (g/m^2/d)	**CH_4/CO_2** (vol.)	**CH_4** (g/m^2/d)	**CO_2** (g/m^2/d)	**CH_4/CO_2** (vol.)
n	27	27	#	94	94	#	69	69	#
Mean	19316.77	434.20	189.28	2.28	10.67	2.90	2.25	23.19	1.01
SD	50472.06	826.42	435.25	0.64	30.71	7.35	0.47	20.27	1.88
Min	6.78	1.66	0.72	2.17	0.09	0.02	2.17	0.44	0.06
Max	241259.24	3066.10	2231.28	6.75	296.22	61.65	5.27	86.66	12.66
Median	1632.37	152.32	88.52	2.17	5.43	1.09	2.17	20.10	0.30
CV	261.29	190.33	229.96	28.07	287.72	253.78	20.99	87.39	187.07
Skewness	3.87	2.71	#	6.01	8.85	6.26	5.88	1.24	4.18
Partial budget (t/yr)	5.71	0.13		9.04*	42.30*		164.49§	1698.92§	
Partial budget (tCO_2-eq/yr)	159.34	0.13		252.34	42.30		4589.35	1698.92	
TOTAL budget (tCO_2-eq/yr)	159.47			294.63			6288.26		

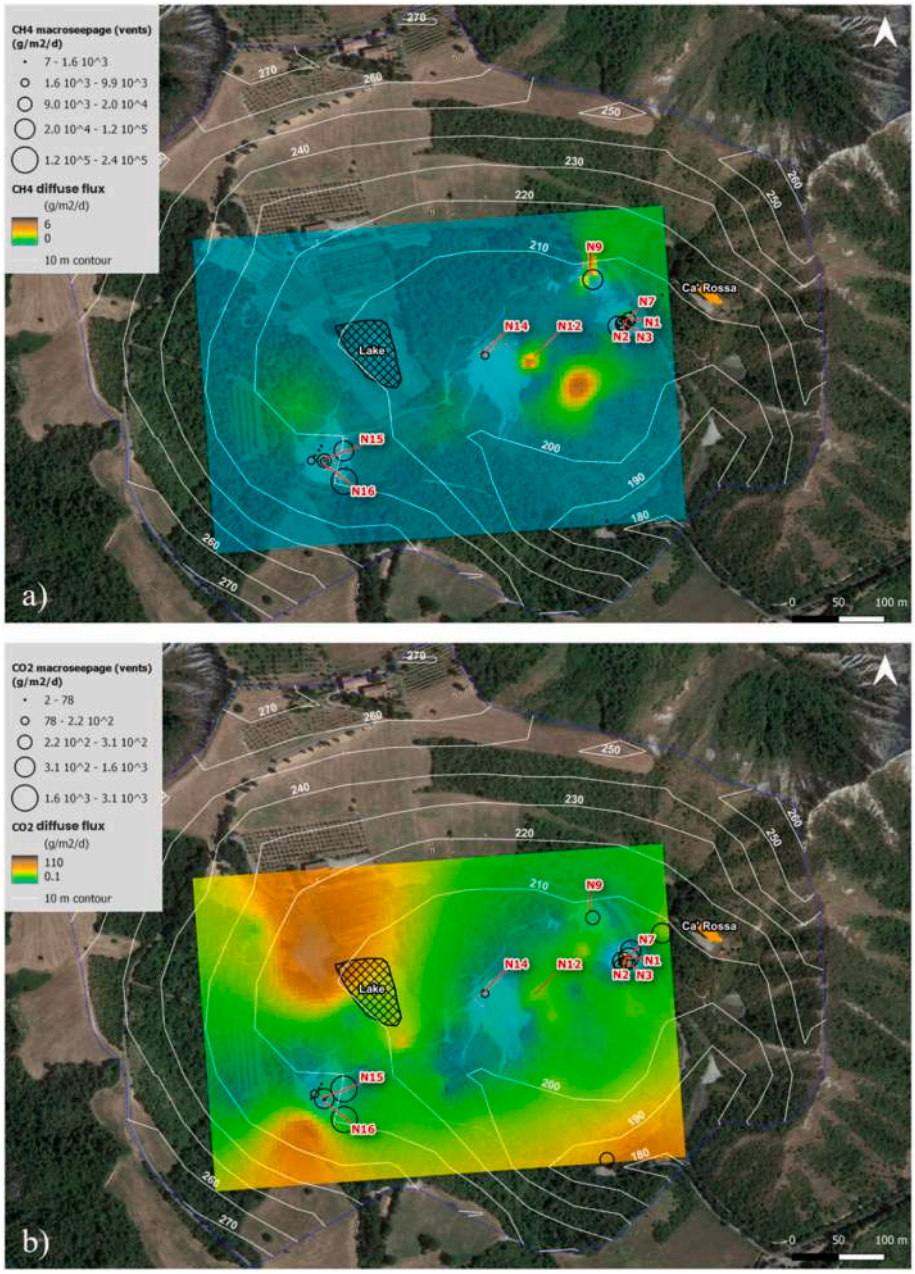

Fig. 5. CH_4 (a) and CO_2 (b) seepage maps. The direct fluxes from the vents are shown by black circles with size proportional to the emission rates.

the cones. Based on the aforementioned considerations, especially points 2 and 4, for the comparison with previous studies, it is preferable to rely on the specific flux of CH_4, which is the total output divided by the investigated area. The CH_4 specific flux is found to be 8.9×10^2 t/km^2/yr, consistent with the 3.2 10^3 t/km^2/yr reported for the Nirano field in Etiope et al. (2007a,b) and the range of 10^2-10^3 t/km^2/yr for mud volcanoes (Etiope et al., 2008; Etiope and Milkov, 2004). We believe that another possible explanation for the difference in CH_4 diffuse flux compared to previous studies is the use of a constant value of 0.10 mol/m^2/d for all flows below the detection limit of the CH_4 detector of the flow chamber (0.2 mol/m^2/d). This substitution may introduce biases in the overall estimate, especially when very low flows constitute a significant percentage of the microseepage database (more than 90%; Fig. 2S in Supplementary Material). It should be noted that the CH_4 estimate, based on the raw data without applying this substitution, indicates a microseepage of 19.8 t/yr, which aligns closely with the findings of previous monitoring conducted by Etiope et al. (2007a, b).

The gas flows measured at the single volcano vent using the flow chamber are similar (N14 = 0.10, N1 = 0.21, and N3 = 0.19 t/yr) to those estimated based on bubble frequency and hydrostatic pressure variation measured through level-loggers with 1-sec interval monitoring (par. 3.2). It must be considered that minor differences can be due to the different methods of acquisition. In fact, the single gryphons are affected by significant macroseepage, characterized by bubbling at different periods (Table 1). This behavior can be captured by long-term monitoring (1-h with 1-sec intervals, Fig. 4), but it cannot be accurately represented by the flow chamber (short-term monitoring). For instance, flow chamber can get saturated in a few minutes (even less than 1 min) in the case of a large gas bubble ascent, resulting in higher flux estimates compared to those obtained by long-term monitoring (i.e. N1 and N3 in Fig. 4); alternatively, the short-term monitoring might not measure the ascent of the largest bubbles that have long periods (i.e. N14 in Table 1) resulting into smaller flux compared to those estimated by long-term

monitoring. These issues should be considered for a more accurate assessment of the gas budget.

CH_4 and CO_2 macroseepage fluxes have the same spatial pattern (cfr. circle symbols in Fig. 5a and b). The highest CH_4/CO_2 ratios are recorded in the vicinity of the active vents and their immediate surroundings. Here the wet mud is not impermeable to gas exhalation and gas flow is rapid enough to continuously replace CH_4 preventing significant oxidation. The CH_4/CO_2 ratios are low in the diffuse microseepage from the soil far from the gryphons and pools, where CH_4 is consumed by methanotrophic bacteria and biologic CO_2 is added by soil respiration (Etiope et al., 2011), resulting in a lower flux ratio (median 0.3) than in the macroseepage (median 88.5).

The estimated GHG emissions are approximately 6.7 10^3 tCO_2-eq/yr (Table 2), a negligible amount compared to the estimates of global natural methane emissions (GEM) of around 40–60 Mt/yr that are produced within the Earth's crust and released naturally into the atmosphere through faults and fractured rocks (Etiope et al., 2011; Etiope, 2005; Mazzini et al., 2021b). Considering the Emilia-Romagna Region (Fig. 6a), the Nirano area emits 0.1% of the total GHGs with the energy and agricultural sector being the most impactful, while in the Modena (Fig. 6b) municipal territory, the emissions from the Nirano reserve account for approximately 2%, with the energy and waste sector being the most impactful. It would be important, in the future, to add to the GEM of Nirano also that of other localities hosting vents and gas seeps within the Emilia Romagna Region to provide a complete picture at regional level.

4.2. Structural data interpretation in connection with gas emissions

Structural data from our geologic survey, surface gas emissions, and available geologic maps (Gasperi et al., 2005) as well as recently published dipole-dipole electric tomography (see Figs. 8, 9, and 10 in Romano et al., 2023) and gravimetry data by Nespoli et al. (2023) are presented in the map of Fig. 7 and in Fig. 3S. The map combined with the orientation data and geologic domains subdivision in Fig. 3 shows the role of fractures and faults to carry the fluids, the role of faults in the Epiligurian sequence in forming the grain of the conduit network and the partially sealing behaviour of the Pliocene FAA. This interpretation is supported by the location of the macroseepage vents, the local stratigraphy, and the pattern of faults, which are present below the *Argille Azzurre* clays in the Pre-Pliocene sequence.

Gas and fluid emissions (Fig. 5) are focalized at points (mud volcanoes) with little or no distributed microseepage. They appear to align in an NE-SW to NNE-SSW direction, which is a secondary structural trend in the pre-Pliocene sequence (Figs. 3, 5 and 7) and that is also similar to the direction of the maximum principal compression direction (N-NNE) in this area of the Apennines (Bonini, 2008). The surface venting could be located at the intersections between the NNE-SSW and NW-SE structural trends being the second the most developed in the pre-Pliocene (Fig. 7). The NW-SE structural is associated with normal faulting as imaged in the geoelectric tomography (Romano et al., 2023), the trend of the geomorphological benches south of the *Nirano Salse* crater (Fig. 1), and the gravimetry (Fig. 3S) (Nespoli et al., 2023), whereas the NNE-SSW trend could be related to transfer or strike-slip faults at high angle to the Northern Apennines fold axis (Fig. 7) as proposed by Vannoli et al. (2021) (see also top inset in Fig. 7). These observations also support the hypothesis of Sciarra et al. (2017) suggesting that the presence of gas flow positive anomalies indicate the existence of highly permeable escape paths connected to deeper layers, likely related to the presence of preferential gas migration pathways such as fractures and/or faults. The flow distribution maps by Sciarra et al. (2019) highlight, according to the authors, the presence of more intense degassing along the morphological edges of the caldera. These areas are positively correlated with the anomalies mapped by Lupi et al. (2016). Our data, along with geoelectric tomographies published by Romano et al. (2023) and the results of Giambastiani et al. (2022), indicate that there is not a widespread diffusion of gases from deep reservoirs, but rather preferential migration along pathways with potential buffering in small shallow aquifers (4–20 m), where the ascending gas is temporarily trapped and stored thanks to the good sealing of clay deposits (FAA Figs. 1 and 7) with discrete conduits where fluids flow upward. The size of the shallow aquifers and syphons along faults or faults intersections may also control the periodicity of large gas bubbles ascent at some vents (i.e. N14 see Fig. 4 and Table 1).

CO_2 macroseepage is low compared to CH_4 macroseepage (Table 1), confirming Nirano as a field of CH_4-rich mud volcanoes like many terrestrial mud volcanoes in Italy (Etiope et al., 2007a,b), and around the world (Japan: Etiope et al., 2011; Taiwan: Chao et al., 2010;

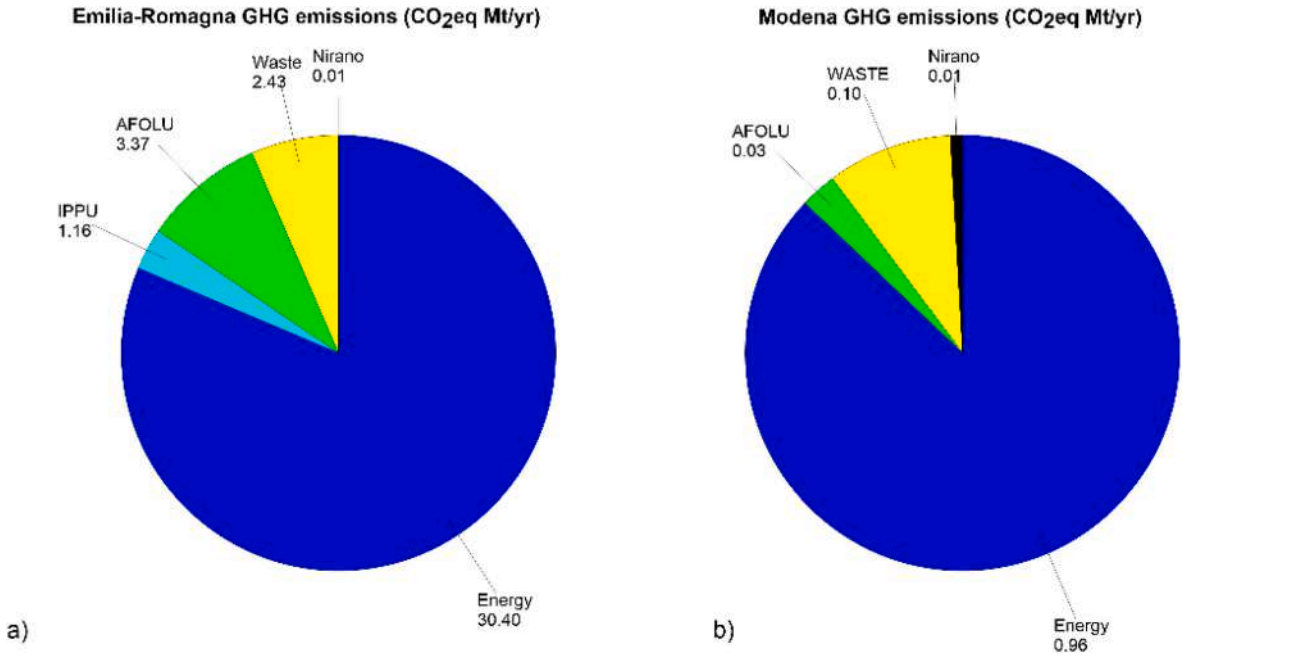

Fig. 6. (a) Regional- (Emilia-Romagna) and (b) municipal- (Modena) scale GHG emission budget.

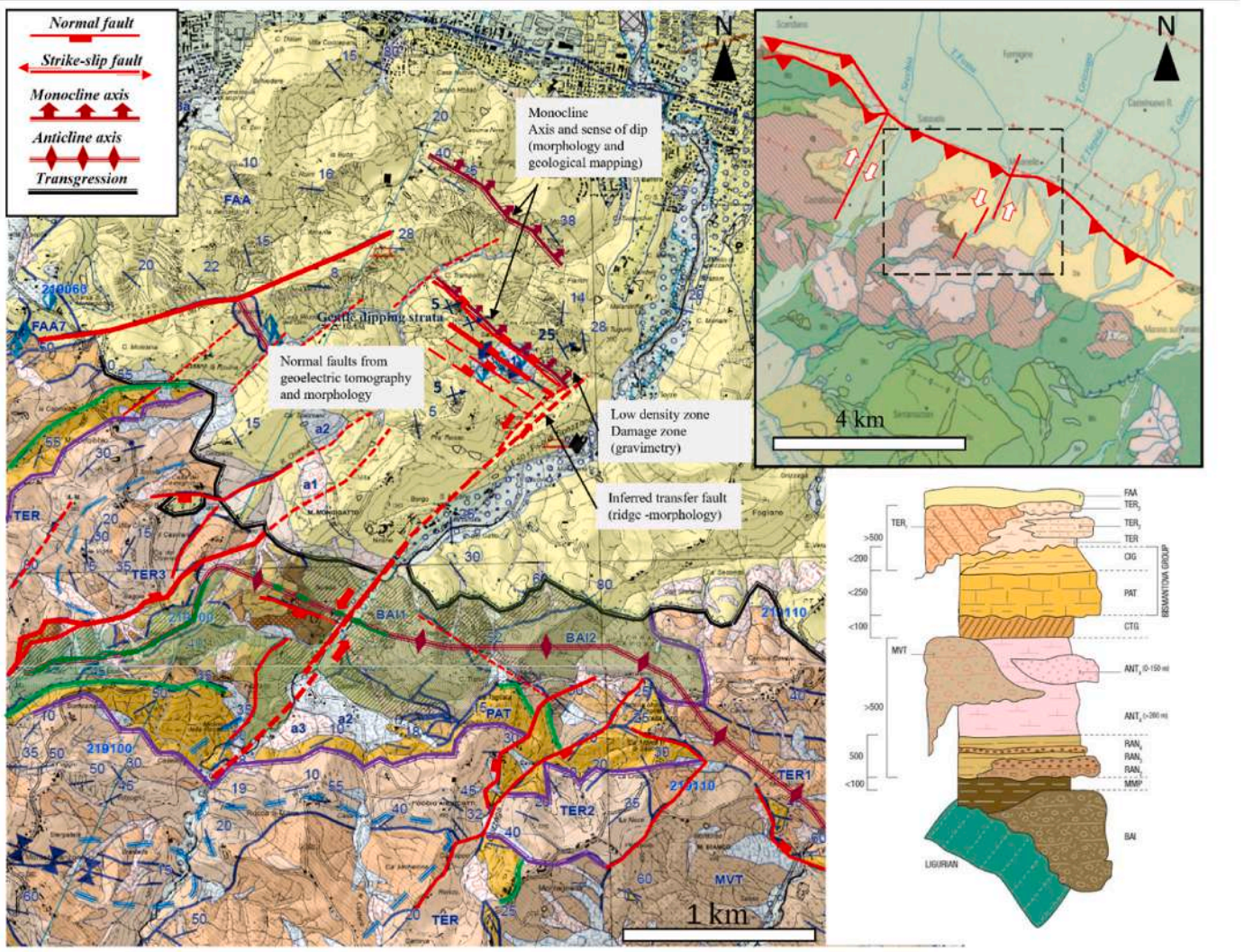

Fig. 7. Geologic map with our data compilation (original scale 1:50000 geology from Emilia-Romagna Region Gasperi et al., 2005, modified in this work) and new structural, geochemical and geophysical observations from this study. The dashed area in the schematic tectonic map of the central portion of the Northern Apennines (top right corner) corresponds to the area covered by the geologic map. Shown is also the stratigraphic profile (details and legend in Fig. 1S in Suppl. Mat.). In red are the faults in the Pre-Pliocene sequence that may play a role in the ascent of deep fluids; dashed where inferred or imaged below the Pliocene sequence. The left-lateral strike-slip fault in the middle of the map allows transfer between two segments of the Apennines chain with different shortening (see inset in the top right corner). The monocline axes (dark red) are shown with a composite line and the sense of dip is represented by the arrows. Strike and dip of strata are also added by the geologic survey conducted during this study (blue dip signs). Normal faults (right red) showing the downthrown side with a solid rectangle are mapped using the geoelectric tomography data of Romano et al. (2023). Strike-slip inferred transfer faults (dashed red lines) are also shown with their sense of slip. The low-density zone mapped by gravimetry by Nespoli et al. (2023) is highlighted by a semitransparent light blue polygon.

Romania: Etiope et al., 2004). The high CH_4/CO_2 ratio confirms the main thermogenic origin of methane ('thermogenic with oil' as indicated in Etiope et al., 2007a,b), which is produced in deep reservoirs (depth >2000 m) along the Apennine sector. These reservoirs are crossed by active and permeable faults through which the CH_4 gas ascends, passing through the Epiligurian units (carbonate marls) and joining some CO_2.

4.3. Strike-slip setting for diapir/seal breakage localization

Recent gravimetric data from Nespoli et al. (2023) show the existence of a NW-SE oriented 250 m wide low-density zone that extends down to a depth of 800 m in the northern portion of the *Nirano Salse* (Figs. 8 and 3S in this work and Fig. 4a in Nespoli et al. (2023)). This low-density zone is also imaged by the geoelectric ERT geo-tomographies published by Romano et al. (2023) (8b in this work and Figs. 8–10 in Romano et al., 2023). Based on the characteristics of the gravimetric and resistivity anomalies, Nespoli et al. (2023) interpret the low-density zone as the damage zone of a sub-vertical NW-SE oriented normal fault invaded by gas and mud (Figs. 8c and 3S in this work and Fig. 4a in Nespoli et al., 2023). The NW-SE structural trend is characteristic in this area of the Apennines and may represent fold axes or normal fault developed in the extrados of the folds following orogenic collapse (Gasperi et al., 2005; Vannoli et al., 2021) or deformation at the extensional quadrant of a strike-slip fault.

On the other hand, the Northern Apennines fold and thrust belt is crossed by NE-SW to ENE-WSW oriented lineaments likely connected to transfer faults accommodating different amounts of shortening in different segments of the belt (Vannoli et al., 2021). In the area next to the *Nirano Salse*, we can recognize the extension of one of these NE-SW to ENE-WSW lineaments (ridge in Fig. 7) that we interpret as a transfer fault with a likely left-lateral strike-slip motion; the fault morphology is apparent in the pre-Pliocene sequence and is concealed below the FAA. The *Nirano Salse* is just west of this structure (Fig. 7 and sketches in

Fig. 8) that also cuts abruptly the NW-SE trending low-density anomaly imaged by the gravimetry in Fig. 3S. Steps along strike-slip faults are areas of stress concentration (Martel and Pollard, 1989) and could localize extension at the tip of the strike-slip faults. The Nirano area, therefore, could undergo local transtension in a general contractional setting (Fig. 8). The transfer structures and the local stress field at their terminations may generate fractures that can be exploited by the fluids to leak off the folded structural traps (NW-SE-oriented) and ascend through the sedimentary sequence and cross the FAA seal where this is thin such at the *Nirano Salse*. At the *Nirano Salse*, the local tensional regime at the tip of a left-lateral strike-slip segment may form NW-SE trending normal faults (as observed in the geophysics) and NE-SW-oriented fractures, which are associated to the strike-slip damage zone. NE-SW-oriented open fractures are regionally present in the Northern Apennines (Gasperi et al., 2205). At the intersections of these two trends, fluid ascent may be particularly easy with the vents generally aligning NE-SW that is not far from the S_H direction. The structural interpretation of the Nirano gas seep and dynamics in Fig. 8 is also in accordance with the interpretative model based on seismic monitoring of gas emission proposed by Carfagna et al. (2024) who suggest a possible dynamical connection between gas emission and seismic signals. The anomalies of the seismic waves at different depth ranges (from 0 to 2–30 m deep) exhibit a trend that mirrors that of the faults we propose (Fig. 8 in this paper and Fig. 8 in Carfagna et al., 2024).

An alignment of gas emissions along a NE-SW structural trend, which could be related to a strike-slip fault, is also reported in the Montegibbio area a few kilometers NW of the *Nirano Salse* (Vannoli et al., 2021). In this latter area, gas and hydrocarbon venting at the surface is reported both in the pre-Pliocene sequence and in the FAA.

Mud volcanoes associated with gas and hydrocarbon emissions along strike-slip faults are reported also in many areas around the world such as the west Moroccan continental margin (Gardner, 2001), the right lateral strike-slip fault system in the Gulf of Cadiz (Hensen et al., 2015; Medialdea et al., 2009; Pérez-Belzuz et al., 1997), along the Central Mediterranean ridge (Huguen et al., 2004), at the Lusi mud Volcano (Mazzini et al., 2009), in the Barbados accretionary wedge (Sumner and Westbrook, 2001), offshore SW Africa (Viola et al., 2005), and in the Mangapakeha mud volcanoes in New Zealand (Zeyen et al., 2011). It appears, therefore, that strike-slip fault systems both in compressional and extensional environments could also be preferential pathways for fluid venting at the Earth's surface.

5. Conclusions

The integrated structural and geochemical study of the *Nirano Salse* that we carried out allows us to propose the following conclusions regarding structural setting, fluid dynamics, and GHG contribution to the carbon budget.

The total actual gas output flux from a mud volcano field cannot be evaluated just by the visible vents (mud pools, gryphons, dry seeps, etc.) but also in the surrounding soil, including the soil and the freshly deposited mud close to the active vents. The wet and dry mud deposits next to the macroseeps are not completely permeable to gas flux and diffusion. Mini- and micro-seepage spread over thousands of m^2 and the total output of gas to the atmosphere is higher than that from focused visible emissions. The diffuse flux could give some hints about the quality of the top seal thickness and integrity; the lower the micro-seepage the thicker and good quality the seal, the higher the micro-seepage the thinner and poor quality the seal.

CO_2 flux at the macroseeps is low compared to CH_4 flux. The specific flux of CH_4 is 8.9 10^2 t/km^2/yr and the volumetric CH_4/CO_2 ratio at the sampling points confirm that the *Nirano Salse* are CH_4-rich of deep thermogenic origin.

The estimated GHG emissions of the *Nirano Salse* are approximately 6.7 10^3 tCO_2-eq/yr, which constitutes 0.1% of the total GHG emission budget of the Emilia-Romagna Region and Modena municipality and it is a negligible amount compared to the estimates of global natural methane emissions that are produced within the Earth crust and released naturally into the atmosphere through faults and fractured rocks.

Surface venting is associated with preferential flow pathways along structural elements or at their intersection as suggested by both geological observations and published recent geophysical surveys (geoelectric tomography and gravimetry). Extensive faulting and fracturing in the pre-Pliocene sequence appear to isolate faulted blocks along which fluids from depth can ascend to the surface. The blanket of *Argille Azzurre* clays seals these fluids that can collect at its base and then break to the surface along pipe-like conduits once the fluid pressure builds up enough to overcome the seal.

The plumbing system of the *Nirano Salse* and its connection with a deep hydrocarbon reservoir is complicate and a matter of current debate; definitely it will still require further detailed geophysical and geologic studies. Here we propose a structural interpretation, which is supported by geophysical, geochemical, and gas flux data and hinges on the following elements: (1) The alignment of the surface vents with a NE-SW to ENE-WSW direction that may represent a local transfer strike-slip structural element in a compressional thrust folds setting. (2) Flexural slip associated with extension at the extrados of an anticline and/or stress concentration at individual transfer (strike-slip) fault segments promote the formation of localized extensional structures (strike NW-SE parallel to the chain) that facilitate deep fluids (CH_4 and liquid hydrocarbons) ascent along faults and fractures of the pre-Pliocene sequence. Small pull-apart structures and different orientation sets of fractures could focus vertical fluid flow. (3) The ductile FAA acts as a top seal and where more permeable (at the base or in constrained lenses) allows the formation of shallow reservoirs. The thinness of the FAA does not guarantee good integrity and fluids from the shallow reservoirs may easily pierce their way to the surface along pipe-like conduits located below the mud vents. (4) The major accumulation of mud and gas is probably in the damage zone of a NW-SE oriented normal fault as suggested by the geophysical and field data.

The implications of our work are important for a series of issues: (1) The correct definition and the weight contribution to the carbon budget of natural gas emissions in a natural reserve such as the *Nirano Salse*. (2) The limitations of various measurement approaches employed in gas emission from mud volcanoes where diverse factors such as flow rates, instrument detection limits, and variations in environmental conditions can impact measurement outcomes. This highlights the necessity to adopt a comprehensive and integrated approach that combines various measurement techniques to better understand the complex dynamics associated with mud volcanoes. (3) The quality of the clay *Argille Azzurre* seal in capping ascending fluids, which is mostly a function of its thickness. (4) The interplay of pre-Pliocene faults that along them or at their intersection form conduits for fluid ascents. (5) The role of strike-slip or transfer faults and their terminations or overlaps to localize surface fluid venting in a compressional environment. (6) Different sizes and periodicity observed for gas bubbles at macroseeps that may point to different conduit shape and size. Continuous high frequency small volume bubbles would be related to rather straight and deep conduits whereas low frequency large volume bubbles could be related to more tortuous paths in syphoned conduits. (7) The economic and risk factors associated with the fruition of the area by tourists. In fact, the information at (3), (4), and (5) could be used to better plan access route to the mud volcanoes and fence off those areas that are prone to surface caving in a way to improve site safety and better promote geo-tourism.

CRediT authorship contribution statement

B.M.S. Giambastiani: Writing – review & editing, Writing – original draft, Visualization, Methodology, Investigation, Data curation, Conceptualization. **E. Chiapponi:** Methodology, Investigation, Data curation. **F. Polo:** Methodology, Data curation. **M. Nespoli:** Visualization, Software, Data curation. **A. Piombo:** Project administration,

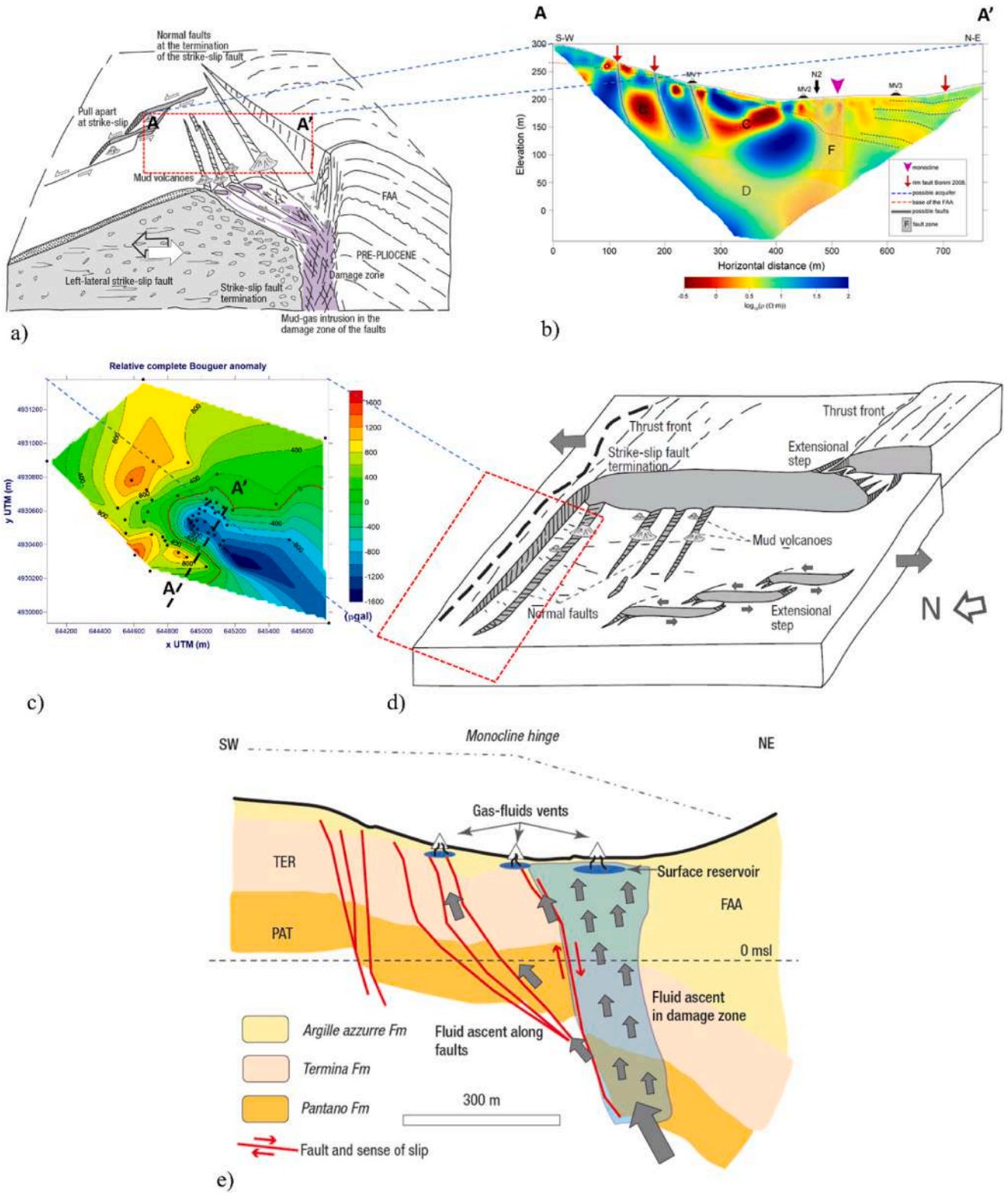

Fig. 8. Structural interpretation of the Nirano gas seep and dynamics. (a) A schematic cross-section in a SW-NE direction that summarizes the data collected from ERT electric geo-tomography from Romano et al. (2023) (b), and relative Bouguer anomaly gravity data (c) from Nespoli et al. (2023); (b) ERT dipole-dipole inversion of geo-tomographic data showing small normal faults and shallow reservoirs associated with surface fluid vents. The area of fluid intrusions to the NE is imaged by low-resistivity data (modified from Romano et al., 2023). (c) Relative complete Bouguer anomaly in the area shown by the red dashed rectangle in (d). Note the NW-SE aligned low-density anomaly that is interpreted as fluid ascent and intrusion along a NW-SE-oriented normal fault developed at the termination of a NE-SW trending left lateral strike-slip transfer fault shown in (d). All normal faults develop in the tensional quadrant of the strike-slip fault. (d) Schematic sketch that shows the structural complexity of the area where a left-lateral strike-slip transfer fault accommodates different shortening among two segments of the Apennines chain; at the tip of a transfer segment intense concentration causes normal faulting to develop. (e) Schematic interpretation of ERT section at (b), which shows the mechanism of fluids ascent at Nirano.

Investigation, Data curation. **M. Antonellini:** Writing – review & editing, Writing – original draft, Validation, Supervision, Resources, Methodology, Investigation, Formal analysis, Data curation, Conceptualization.

Declaration of competing interest

The authors declare that they have no known competing financial interests or personal relationships that could have appeared to influence the work reported in this paper.

Data availability

Data will be made available on request.

Acknowledgements

This study was performed with the support of the Fiorano Modenese Municipality (Italy) and the Management Authority for Park and Biodiversity of Central Emilia (Ente di Gestione per i Parchi e la Biodiversità Emilia Centrale, Italy). The authors thank Luciano Callegari, Marzia Conventi and Maria Morena for their support in the logistics and the warm welcome. The reviews of Marco Bonini, Davide Oppo, and Alessandra Sciarra have greatly contributed to the improvement of our manuscript.

Appendix A. Supplementary data

Supplementary data to this article can be found online at https://doi.org/10.1016/j.marpetgeo.2024.106771.

References

Allmendinger, R.W., 2019. Modern Structural Practice - A Structural Geology Laboratory Manual for the 21st Century.

Aminzadeh, F, Berge, TB, Connolly, D.L., 2013. Hydrocarbon seepage: from source to surface. library.seg.org. https://doi.org/10.1190/1.9781560803119.

Amorosi, A., Barbieri, M., Castorina, F., Colalongo, M.L., Pasini, G., Vaiani, S.C., 1998. Sedimentology, micropaleontology, and strontium-isotope dating of a lower-middle Pleistocene marine succession ("Argille Azzurre") in the Romagna Apennines, northern Italy. Boll. Soc. Geol. Ital. 117, 789–806.

Amrikazemi, A., Mehrpooya, A., 2005. Geotourism resources of Iran. In: Geotourism, p. 15.

Bennett, R.A., Serpelloni, E., Hreinsdòttir, S., Brandon, M.T., Buble, G., Basic, T., Casale, G., Cavaliere, A., Anzidei, M., Marjonovic, M., Mineli, G., Molli, G., Montanari, A., 2012. Syn-convergent extension observed using the RETREAT GPS network, northern Apennines, Italy. JGR Solid Earth 117, B04408. https://doi.org/10.1029/2011JB008744.

Bonini, M., 2020. Investigating earthquake triggering of fluid seepage systems by dynamic and static stresses. Earth Sci. Rev. 210, 103343 https://doi.org/10.1016/j.earscirev.2020.103343.

Bonini, M., 2012. Mud volcanoes: indicators of stress orientation and tectonic controls. Earth Sci. Rev. 115, 121–152. https://doi.org/10.1016/j.earscirev.2012.09.002.

Bonini, M., 2009. Mud volcano eruptions and earthquakes in the northern Apennines and sicily, Italy. Tectonophysics 474, 723–735. https://doi.org/10.1016/j.tecto.2009.05.018.

Bonini, M., 2008. Elliptical mud volcano caldera as stress indicator in an active compressional setting (Nirano, Pede-Apennine margin, northern Italy). Geol. 36, 131. https://doi.org/10.1130/G24158A.1.

Bonini, M., 2007. Interrelations of mud volcanism, fluid venting, and thrust-anticline folding: examples from the external northern Apennines (Emilia-Romagna, Italy). J. Geophys. Res. 112, B08413 https://doi.org/10.1029/2006JB004859.

Capaccioni, B., Caramiello, C., Corigliano, G., de Rosa, S., Tatàno, F., Viscione, A., 2010. Monitoring of landfill gas emission rates: application of the static chamber approach to an Italian sanitary landfill site. In: Presented at the WASTE MANAGEMENT 2010, pp. 287–299. https://doi.org/10.2495/WM100261. Tallinn, Estonia.

Capaccioni, B., Tassi, F., Cremonini, S., Sciarra, A., Vaselli, O., 2015. Ground heating and methane oxidation processes at shallow depth in Terre Calde di Medolla (Italy): observations and conceptual model: soil heating due to methane oxidation. J. Geophys. Res. Solid Earth 120, 3048–3064. https://doi.org/10.1002/2014JB011635.

Capozzi, R., Picotti, V., 2010. Spontaneous fluid emissions in the Northern Apennines: geochemistry, structures and implications for the petroleum system. Geological Society, London, Special Publications 348, 115–135. https://doi.org/10.1144/SP348.7.

Capozzi, R., Picotti, V., 2002. Fluid migration and origin of a mud volcano in the Northern Apennines (Italy): the role of deeply rooted normal faults: mud volcanoes and deeply rooted normal faults. Terra. Nova 14, 363–370. https://doi.org/10.1046/j.1365-3121.2002.00430.x.

Cardellini, C., Chiodini, G., Frondini, F., Granieri, D., Lewicki, J., Peruzzi, L., 2003. Accumulation chamber measurements of methane fluxes: application to volcanic-geothermal areas and landfills. Appl. Geochem. 18, 45–54. https://doi.org/10.1016/S0883-2927(02)00091-4.

Carfagna, N., Brindisi, A., Paolucci, E., Albarello, D., 2024. Seismic monitoring of gas emissions at mud volcanoes: the case of Nirano (Northern Italy). J. Volcanol. Geoth. Res. 446, 107993 https://doi.org/10.1016/j.jvolgeores.2023.107993.

Carlini, M., Chelli, A., Vescovi, P., Artoni, A., Clemenzi, L., Tellini, C., Torelli, L., 2016. Tectonic control on the development and distribution of large landslides in the Northern Apennines (Italy). Geomorphology 253, 425–437. https://doi.org/10.1016/j.geomorph.2015.10.028.

Chao, H.-C., You, C.-F., Sun, C.-H., 2010. Gases in Taiwan mud volcanoes: chemical composition, methane carbon isotopes, and gas fluxes. Appl. Geochem. 25, 428–436. https://doi.org/10.1016/j.apgeochem.2009.12.009.

Ciotoli, G., Lombardi, S., Annunziatellis, A., 2007. Geostatistical analysis of soil gas data in a high seismic intermontane basin: fucino Plain, central Italy. J. Geophys. Res. 112, B05407 https://doi.org/10.1029/2005JB004044.

Conti, A., Sacchi, E., Chiarle, M., Martinelli, G., Zuppi, G.M., 2000. Geochemistry of the formation waters in the Po plain (Northern Italy): an overview. Appl. Geochem. 15, 51–65. https://doi.org/10.1016/S0883-2927(99)00016-5.

Etiope, G., 2015. Natural Gas Seepage: the Earth's Hydrocarbon Degassing. Springer International Publishing, Cham. https://doi.org/10.1007/978-3-319-14601-0.

Etiope, G., 2005. Gem - geologic Emissions of Methane, the missing source of the atmospheric methane budget. In: Geophysical Research Abstracts, 03123. Presented at the European Geosciences Union 2005, p. 3.

Etiope, G., Baciu, C., Caracausi, A., Italiano, F., Cosma, C., 2004. Gas flux to the atmosphere from mud volcanoes in eastern Romania. Terra. Nova 16, 179–184. https://doi.org/10.1111/j.1365-3121.2004.00542.x.

Etiope, G., Feyzullayev, A., Milkov, A.V., Waseda, A., Mizobe, K., Sun, C.H., 2009. Evidence of subsurface anaerobic biodegradation of hydrocarbons and potential secondary methanogenesis in terrestrial mud volcanoes. Mar. Petrol. Geol. 26, 1692–1703. https://doi.org/10.1016/j.marpetgeo.2008.12.002.

Etiope, G., Fridriksson, T., Italiano, F., Winiwarter, W., Theloke, J., 2007a. Natural emissions of methane from geothermal and volcanic sources in Europe. J. Volcanol. Geoth. Res. 165, 76–86. https://doi.org/10.1016/j.jvolgeores.2007.04.014.

Etiope, G., Lassey, K.R., Klusman, R.W., Boschi, E., 2008. Reappraisal of the fossil methane budget and related emission from geologic sources. Geophys. Res. Lett. 35, L09307 https://doi.org/10.1029/2008GL033623.

Etiope, G., Martinelli, G., Caracausi, A., Italiano, F., 2007b. Methane seeps and mud volcanoes in Italy: gas origin, fractionation and emission to the atmosphere. Geophys. Res. Lett. 34, L14303 https://doi.org/10.1029/2007GL030341.

Etiope, G., Milkov, A.V., 2004. A new estimate of global methane flux from onshore and shallow submarine mud volcanoes to the atmosphere. Environ. Geol. (Berl.) 46, 997–1002. https://doi.org/10.1007/s00254-004-1085-1.

Etiope, G., Nakada, R., Tanaka, K., Yoshida, N., 2011. Gas seepage from Tokamachi mud volcanoes, onshore Niigata Basin (Japan): origin, post-genetic alterations and CH4–CO2 fluxes. Appl. Geochem. 26, 348–359. https://doi.org/10.1016/j.apgeochem.2010.12.008.

Etiope, G., Sherwood Lollar, B., 2013. Abiotic methane on earth: abiotic methane on earth. Rev. Geophys. 51, 276–299. https://doi.org/10.1002/rog.20011.

Formolo, M., 2010. The microbial production of methane and other volatile hydrocarbons. In: Timmis, K.N. (Ed.), Handbook of Hydrocarbon and Lipid Microbiology. Springer Berlin Heidelberg, Berlin, Heidelberg, pp. 113–126. https://doi.org/10.1007/978-3-540-77587-4_6.

Gardner, J.M., 2001. Mud volcanoes revealed and sampled on the western Moroccan continental margin. Geophys. Res. Lett. 28, 339–342. https://doi.org/10.1029/2000GL012141.

Gasperi, G., 1989. Evoluzione plio-quaternaria del margine appenninico modenese e dell'antistante pianura: note illustrative alla carta geologica. Memorie Società Geologica Italiana 39, 375–431.

Gasperi, G., Bettelli, G., Panini, F., Pizziolo, M., Bonazzi, U., Fioroni, C., Fregni, P., Vaiani, S.C., 2005. Note Illustrative Alla Carta Geologica d'Italia Alla Scala 1:50.000. Foglio 219 "Sassuolo". Regione Emilia – Romagna.

Giambastiani, B.M.S., Antonellini, M., Nespoli, M., Bacchetti, M., Calafato, A., Conventi, M., Dadomo, A., Martinelli, G., Morena, M., Venturoli, S., Piombo, A., 2022. Mud flow dynamics at gas seeps - Nirano Salse, Italy -. Environ. Earth Sci. 81, 480. https://doi.org/10.1007/s12665-022-10615-2.

Giovenali, E., Coppo, L., Virgili, G., Continanza, D., Raco, B., 2013. The Flux-Meter: Implementation of A Portable Integrated Instrumentation for the Measurement of Co2 and Ch4 Diffuse Flux from Landfill Soil Cover.

Heller, C., Blumenberg, M., Hoppert, M., Taviani, M., Reitner, J., 2012. Terrestrial mud volcanoes of the Salse di Nirano (Italy) as a window into deeply buried organic-rich shales of Plio-Pleistocene age. Sediment. Geol. 263 (264), 202–209. https://doi.org/10.1016/j.sedgeo.2011.05.004.

Heller, C., Blumenberg, M., Kokoschka, S., Wrede, C., Hoppert, M., Taviani, M., Reitner, J., 2011. Geomicrobiology of fluid venting structures at the Salse di Nirano Mud Volcano area in the northern Apennines (Italy). In: Advances in Stromatolite Geobiology, Lecture Notes in Earth Sciences. Springer Berlin Heidelberg, Berlin, Heidelberg, pp. 209–220. https://doi.org/10.1007/978-3-642-10415-2_14.

Hensen, C., Scholz, F., Nuzzo, M., Valadares, V., Gràcia, E., Terrinha, P., Liebetrau, V., Kaul, N., Silva, S., Martínez-Loriente, S., Bartolome, R., Piñero, E., Magalhães, V.H., Schmidt, M., Weise, S.M., Cunha, M., Hilario, A., Perea, H., Rovelli, L.,

Lackschewitz, K., 2015. Strike-slip faults mediate the rise of crustal-derived fluids and mud volcanism in the deep sea. Geology 43, 339–342. https://doi.org/10.1130/G36359.1.
Herrera-Franco, G., Carrión-Mero, P., Alvarado, N., Morante-Carballo, F., Maldonado, A., Caldevilla, P., Briones-Bitar, J., Berrezueta, E., 2020. Geosites and georesources to foster geotourism in communities: case study of the santa elena peninsula geopark project in Ecuador. Sustainability 12, 4484. https://doi.org/10.3390/su12114484.
Hmiel, B., Petrenko, V.V., Dyonisius, M.N., Buizert, C., Smith, A.M., Place, P.F., Harth, C., Beaudette, R., Hua, Q., Yang, B., Vimont, I., Michel, S.E., Severinghaus, J.P., Etheridge, D., Bromley, T., Schmitt, J., Faïn, X., Weiss, R.F., Dlugokencky, E., 2020. Preindustrial 14CH4 indicates greater anthropogenic fossil CH4 emissions. Nature 578, 409–412. https://doi.org/10.1038/s41586-020-1991-8.
Howarth, R.W., 2014. A bridge to nowhere: methane emissions and the greenhouse gas footprint of natural gas. Energy Sci. Eng. 2, 47–60. https://doi.org/10.1002/ese3.35.
Huguen, C., Mascle, J., Chaumillon, E., Kopf, A., Woodside, J., Zitter, T., 2004. Structural setting and tectonic control of mud volcanoes from the central Mediterranean ridge (eastern mediterranean). Mar. Geol. 209, 245–263. https://doi.org/10.1016/j.margeo.2004.05.002.
Hunt, M., 1996. Co. ed. In: Freeman, W.H. (Ed.), Petroleum Geochemistry and Geology, end ed. New York.
IPCC, 2022. Climate Change 2022: Impacts, Adaptation, and Vulnerability. Contribution of Working Group II to the Sixth Assessment Report of the Intergovernmental Panel on Climate Change. Cambridge University Press, Cambridge, UK and New York, NY, USA. Cambridge University Press.
Kopf, A.J., 2002. Significance of mud volcanism. Rev. Geophys. 40, 1005. https://doi.org/10.1029/2000RG000093.
Kuhn, O., 2000. Odyssey of Oil, vol. 25. RECORDER - Official publication of the Canadian Society of Exploration Geophysicists.
Leroy, S.A.G., Gracheva, R., Medvedev, A., 2022. Natural hazards and disasters around the Caspian Sea. Nat. Hazards 114, 2435–2478. https://doi.org/10.1007/s11069-022-05522-5.
Lupi, M., Ricci, B.S., Kenkel, J., Ricci, T., Fuchs, F., Miller, S.A., Kemna, A., 2016. Subsurface fluid distribution and possible seismic precursory signal at the Salse di Nirano mud volcanic field. Italy. Geophys. J. Int. 204, 907–917. https://doi.org/10.1093/gji/ggv454.
MacDonald, I.R., Buthman, D.B., Sager, W.W., Peccini, M.B., Guinasso Jr., N.L., 2000. Pulsed oil discharge from a mud volcano. Geology 28, 907–910.
Madeja, G., Mrowczyk, P., 2010. Phenomenon of mud volcanoes in western Romania as a geoturism object. In: Presented at the XIX Congress of the Carpathian-Balkan Geological Association Thessaloniki, p. 237. Greece, 23-26 September 2010.
Maestrelli, D., Bonini, M., Sani, F., 2019. Linking structures with the genesis and activity of mud volcanoes: examples from Emilia and Marche (Northern Apennines, Italy). Int. J. Earth Sci. 108, 1683–1703. https://doi.org/10.1007/s00531-019-01730-w.
Manga, M., Bonini, M., 2012. Large historical eruptions at subaerial mud volcanoes, Italy. Nat. Hazards Earth Syst. Sci. 12, 3377–3386. https://doi.org/10.5194/nhess-12-3377-2012.
Mariucci, M.T., Amato, A., Montone, P., 1999. Recent tectonic evolution and present stress in the Northern Apennines (Italy). Tectonics 18, 108–118. https://doi.org/10.1029/1998TC900019.
Martel, S.J., Pollard, D.D., 1989. Mechanics of slip and fracture along small faults and simple strike-slip fault zones in garnitic rock. J. Geophys. Res. 94, 9417–9428.
Martinelli, G., Cremonini, S., Samonati, E., 2012. Geological and geochemical setting of natural hydrocarbon emissions in Italy. In: Al-Megren, H. (Ed.), Advances in Natural Gas Technology. InTech. https://doi.org/10.5772/37446.
Martinelli, G., Judd, A., 2004. Mud volcanoes of Italy. Geol. J. 39, 49–61. https://doi.org/10.1002/gj.943.
Martinelli, G., Rabbi, 1998. The Nirano mud vulcanoes. Abstract and guide book. In: V International Conference on Gas in Marine Sediment, pp. 202–206.
Mattavelli, L., Novelli, L., 1988. Geochemistry and habitat of natural gases in Italy. Org. Geochem. 13, 1–13. https://doi.org/10.1016/0146-6380(88)90021-6.
Mattavelli, L., Pieri, M., Groppi, G., 1993. Petroleum exploration in Italy: a review. Marine and Petroleum Geology 10 (5), 410–425. https://doi.org/10.1016/0264-8172(93)90044-S. ISSN 0264-8172.
Mattavelli, Ricchiuto, Teodoro, G, D., Martin, Schoell, 1983. Geochemistry and habitat of natural gases in Po basin, northern Italy. Bulletin 67. https://doi.org/10.1306/AD46094F-16F7-11D7-8645000102C1865D.
Mazzini, A., Akhmanov, G., Manga, M., Sciarra, A., Huseynova, A., Huseynov, A., Guliyev, I., 2021a. Explosive mud volcano eruptions and rafting of mud breccia blocks. Earth Planet Sci. Lett. 555, 116699 https://doi.org/10.1016/j.epsl.2020.116699.
Mazzini, A., Etiope, G., 2017. Mud volcanism: an updated review. Earth Sci. Rev. 168, 81–112. https://doi.org/10.1016/j.earscirev.2017.03.001.
Mazzini, A., Nermoen, A., Krotkiewski, M., Podladchikov, Y., Planke, S., Svensen, H., 2009. Strike-slip faulting as a trigger mechanism for overpressure release through piercement structures. Implications for the Lusi mud volcano, Indonesia. Mar. Petrol. Geol. 26, 1751–1765. https://doi.org/10.1016/j.marpetgeo.2009.03.001.
Mazzini, A., Sciarra, A., Etiope, G., Sadavarte, P., Houweling, S., Pandey, S., Husein, A., 2021b. Relevant methane emission to the atmosphere from a geological gas manifestation. Sci. Rep. 11, 4138. https://doi.org/10.1038/s41598-021-83369-9.
Medialdea, T., Somoza, L., Pinheiro, L.M., Fernández-Puga, M.C., Vázquez, J.T., León, R., Ivanov, M.K., Magalhaes, V., Díaz-del-Río, V., Vegas, R., 2009. Tectonics and mud volcano development in the Gulf of Cádiz. Mar. Geol. 261, 48–63. https://doi.org/10.1016/j.margeo.2008.10.007.
Minissale, A., Magro, G., Martinelli, G., Vaselli, O., Tassi, G.F., 2000. Fluid geochemical transect in the Northern Apennines (central-northern Italy): fluid genesis and migration and tectonic implications. Tectonophysics 319, 199–222. https://doi.org/10.1016/S0040-1951(00)00031-7.
Nespoli, M., Antonellini, M., Albarello, D., Lupi, M., Cenni, N., Piombo, A., 2023. Gravity data allow to image the shallow-medium subsurface below mud volcanoes. Geophy. Res. Lett. 50 (20), 1–10. https://doi.org/10.1029/2023GL103505.
Oertel, C., Matschullat, J., Zurba, K., Zimmermann, F., Erasmi, S., 2016. Greenhouse gas emissions from soils- a review. Geochemistry 76 (3), 327–352. https://doi.org/10.1016/j.chemer.2016.04.002.
Oppo, D., Capozzi, R., Picotti, V., 2013. A new model of the petroleum system in the Northern Apennines, Italy. Mar. Petrol. Geol. 48, 57–76. https://doi.org/10.1016/j.marpetgeo.2013.06.005.
Oppo, D., Viola, I., Capozzi, R., 2017. Fluid sources and stable isotope signatures in authigenic carbonates from the Northern Apennines, Italy. Mar. Petrol. Geol. 86, 606–619. https://doi.org/10.1016/j.marpetgeo.2017.06.016.
Orange, D.L., Greene, H.G., Reed, D., Martin, J.B., McHugh, C.M., Ryan, W.B.F., Maher, N., Stakes, D., Barry, J., 1999. Widespread fluid expulsion on a translational continental margin: mud volcanoes, fault zones, headless canyons, and organic-rich substrate in Monterey Bay, California. GSA Bulletin 111, 992–1009.
Pallasser, R.J., 2000. Recognising biodegradation in gas/oil accumulations through the δ13C compositions of gas components. Organic Geochemistry 31 (12), 1363–1373. ISSN 0146-6380. https://doi.org/10.1016/S0146-6380(00)00101-7.
Papazzoni, 2017. Studio micropaleontologico dei fanghi delle Salse di Nirano. Atti della Soc. dei Nat. Mat. Modena 121–126.
Pérez-Belzuz, F., Alonso, B., Ercilla, G., 1997. History of mud diapirism and trigger mechanisms in the Western Alboran Sea. Tectonophysics 282, 399–422. https://doi.org/10.1016/S0040-1951(97)00226-6.
Picotti, V., Capozzi, R., Bertozzi, G., Mosca, F., Sitta, A., Tornaghi, M., 2007. The Miocene petroleum system of the northern Apennines in the central Po plain (Italy). In: Lacombe, O., Roure, F., Lavé, J., Vergés, J. (Eds.), Thrust Belts and Foreland Basins, Frontiers in Earth Sciences. Springer Berlin Heidelberg, Berlin, Heidelberg, pp. 117–131. https://doi.org/10.1007/978-3-540-69426-7_6.
Riva, A., Salvatori, T., Cavaliere, R., Ricchiuto, T., Novelli, L., 1986. Origin of oils in Po Basin, Northern Italy. Organic Geochemistry 10 (1–3), 391–400. ISSN 0146-6380. https://doi.org/10.1016/0146-6380(86)90038-0.
Romano, G., Antonellini, M., Patella, D., Siniscalchi, A., Tallarico, A., Tripaldi, S., Piombo, A., 2023. Fluid conduits and shallow-reservoir structure defined by geoelectrical tomography at the Nirano Salse (Italy). Nat. Hazards Earth Syst. Sci. 23, 2719–2735. https://doi.org/10.5194/nhess-23-2719-2023.
Sciarra, A., Cantucci, B., Castaldini, D., Procesi, M., Conventi, M., 2015. Between history, work and passion: medieval castle, mud volcanoes and Ferrari. Goldschmidt Conference - Fiorano Modenese, 2013. ISPRA Technical Periodicals - Geological Field Trips and Maps 7 (1.1), 42. https://doi.org/10.3301/GFT.2015.01.
Sciarra, A., Cantucci, B., Conventi, M., Ricci, T., 2017. Caratterizzazione geochimica e monitoraggio dei flussi e delle componenti gassose nella Riserva delle Salse di Nirano. In: Studi interdisciplinari in Scienze della Terra per la fruizione in sicurezza della Riserva Naturale delle Salse di Nirano. Atti Soc. Nat. Mat., Modena, pp. 79–98.
Sciarra, A., Cantucci, B., Ricci, T., Tomonaga, Y., Mazzini, A., 2019. Geochemical characterization of the Nirano mud volcano, Italy. Appl. Geochem. 102, 77–87. https://doi.org/10.1016/j.apgeochem.2019.01.006.
Serpelloni, E., Anzidei, M., Baldi, P., Casula, G., Galani, A., 2015. Crustal velocity and strain-rate fields in Itay and surrounding regions: new results from the analysis of permanent and non-permanent GPS networks. Geophys. J. Int. 161 (3), 861–880. https://doi.org/10.1111/j.1365-246X.2005.02618.x.
Stendardi, F., Viola, G., Vignaroli, G., 2023. Multiscale structural analysis of an Epiligurian wedge-top basin: insights into the syn- to post-orogenic evolution of the Northern Apennines accretionary wedge (Italy). Int. J. Earth Sci. 112, 805–827. https://doi.org/10.1007/s00531-022-02286-y.
Sumner, R.H., Westbrook, G.K., 2001. Mud diapirism in front of the Barbados accretionary wedge: the influence of fracture zones and North America–South America plate motions. Mar. Petrol. Geol. 18, 591–613. https://doi.org/10.1016/S0264-8172(01)00010-1.
Tassi, F., Bonini, M., Montegrossi, G., Capecchiacci, F., Capaccioni, B., Vaselli, O., 2012. Origin of light hydrocarbons in gases from mud volcanoes and CH4-rich emissions. Chem. Geol. 294–295, 113–126. https://doi.org/10.1016/j.chemgeo.2011.12.004.
Vannoli, P., Martinelli, G., Valensise, G., 2021. The seismotectonic significance of geofluids in Italy. Front. Earth Sci. 9, 579390 https://doi.org/10.3389/feart.2021.579390.
Viola, G., Andreoli, M., Ben-Avraham, Z., Stengel, I., Reshef, M., 2005. Offshore mud volcanoes and onland faulting in southwestern Africa: neotectonic implications and constraints on the regional stress field. Earth Planet Sci. Lett. 231, 147–160. https://doi.org/10.1016/j.epsl.2004.12.001.
Wan, Z., Zhang, J., Lin, G., Zhong, S., Li, Q., Wei, J., Sun, Y., 2021. Formation mechanism of mud volcanoes/mud diapirs based on physical simulation. Geofluids 2021, 1–16. https://doi.org/10.1155/2021/5531957.
Wang, W., Zhang, L., Liu, W., Kang, Y., Ren, J., 2005. Effects of biodegradation on the carbon isotopic composition of natural gas-A case study in the bamianhe oil field of the Jiyang Depression, Eastern China. Geochem. J. 39, 301–309. https://doi.org/10.2343/geochemj.39.301.
Wang, Y., Lin, Y.N., Ota, Y., Chung, L., Shyu, J.B.H., Chiang, H., Chen, Y., Hsu, H., Shen, C., 2022. Mud diapir or fault-related fold? On the development of an active mud-cored anticline offshore southwestern taiwan. Tectonics 41. https://doi.org/10.1029/2022TC007234.
West Systems, 2012. Portable Flux Meter Handbook - Release, 8.2.

Whiticar, M.J., Suess, E., 1990. Hydrothermal hydrocarbon gases in the sediments of the king george basin, bransfield strait, Antarctica. Appl. Geochem. 5, 135–147. https://doi.org/10.1016/0883-2927(90)90044-6.

Zeyen, H., Pessel, M., Ledésert, B., Hébert, R., Bartier, D., Sabin, M., Lallemant, S., 2011. 3D electrical resistivity imaging of the near-surface structure of mud-volcano vents. Tectonophysics 509, 181–190. https://doi.org/10.1016/j.tecto.2011.05.007.

Zhong, S., Zhang, J., Luo, J., Yuan, Y., Su, P., 2021. Geological characteristics of mud volcanoes and diapirs in the northern continental margin of the south China sea: implications for the mechanisms controlling the genesis of fluid leakage structures. Geofluids 2021, 1–17. https://doi.org/10.1155/2021/5519264.